FACULDADE DE ENGENHARIA DO PORTO DA UNIVERSIDADE DO PORTO

Preparation and characterization of porous 3D Bonelike® structures through biomodelling and 3D machining techniques

Marta de Sousa Laranjeira
Licenciada em Biologia Geologia Ensino pela Faculdade de Ciências da Universidade do Porto

Dissertação submetida para satisfação parcial dos
requisitos do grau de mestre
em
Engenharia Biomédica
(Área de especialização Biomateriais)

Dissertação realizada sob a supervisão de
Professor José Domingos da Silva Santos e
Dra. Anabela Gregório Dias
do departamento de Engenharia Metalúrgica e Materiais
da Faculdade de Engenharia da Universidade do Porto

Porto, Dezembro de 2006

Aos meus pais

"…que o sonho comanda a vida, que sempre que um homem sonha, o mundo pula e avança…"

António Gedeão, *Pedra Filosofal*

Resumo

Os biomateriais bioactivos e bioareabsorvíveis podem ser utilizados na cirurgia renegerativa do tecido ósseo, evitando, desta forma, os problemas associados aos autoenxertos, tais como a morbilidade do local de recolha e a quantidade limitada de enxerto ou, no caso dos alloenxertos, a rejeição imunitária e a transmissão patogénica. Com estes biomateriais, é possível construir estruturas tridimensionais (3D), que poderão ser usadas em diversas aplicações médicas de regeneração do tecido ósseo e na engenharia de tecidos.

O objectivo do presente trabalho foi o de desenvolver e optimizar estruturas bioactivas 3D macroporosas com porosidade aberta e interconectiva, adequadas à regeneração do tecido ósseo, que facilitassem a migração de células, ancoramento e crescimento do tecido ósseo no seu interior, bem como a neovascularização do novo osso. A preparação das estruturas tridimensionais teve por base as técnicas de biomodelação 3D e maquinagem 3D. Estas técnicas apresentam vantagens face aos métodos convencionais de preparação de materiais macroporosos, pois permitem que o material seja modelado com uma forma adequada ao local de implantação, para além de um maior controlo da porosidade, do tamanho e distribuição dos poros.

Na primeira parte do trabalho, os biomateriais (hidroxiapatite e Bonelike®) foram preparados em laboratório e caracterizados por diferentes técnicas físico-químicas. Verificou-se que o Bonelike® para além da hidroxiapatite apresentava as fases secundárias β-tricálcio fosfato (β-TCP) e α-tricálcio fostato (α-TCP), resultantes da reacção entre a matriz da hidroxiapatite e o vidro, durante a sinterização, na presença da fase líquida.

Posteriormente, as estruturas tridimensionais foram modeladas por computador, com softwares adequados, e maquinadas através de uma máquina CNC. Foram obtidas estruturas tridimensionais de Bonelike® com macroporosidade controlada. O tamanho dos macroporos obtidos após sinterização foi de, aproximadamente, 2000 μm.

Os estudos biológicos *in vitro* foram realizados com culturas de células humanas da medula óssea, que incluem células capazes de se diferenciar em células da linhagem

óssea. Verificou-se que as células aderiram e proliferaram à superfície e foram igualmente capazes de migrar através dos macroporos da estrutura. Foram também, identificadas estruturas globulares mineralizadas associadas às células, demonstrando que estas se diferenciaram.

Os resultados obtidos indicam que as estruturas 3D de Bonelike® preparadas por maquinagem 3D com porosidade interconnectiva e macroporos de 2 000 μm, permitem com sucesso a migração das células para o interior de todos os macroporos, bem como a proliferação e diferenciação das células humanas da medula óssea.

Abstract

Bioactive and bioresorbable materials can be used in bone regenerative surgery, avoiding autografts limitations, such as donor site morbidity and the limited amount of the graft or, in the case of allograft, the possibility of immune rejection and pathogenic transmission. Using these biomaterials it is possible to construct three-dimensional (3D) structures, which can be used in regenerative bone surgery, as well as scaffolds, for tissue engineering applications.

The aim of the present work was to develop and optimize 3D bioactive macroporous structures with open pores interconnected, appropriate for bone regeneration, allowing cell migration, vascularization and tissue ingrowth. The 3D structures were prepared using 3D Biomodelling and 3D machining techniques.

These techniques show advantages comparing to conventional methods used to prepare macroporous materials. With 3D biomodelling scaffolds can be designed and manufactured according size and conformation of the implant site, with controlled morphology and porosity.

In the first part of the work, the biomaterials (hydroxyapatite and Bonelike®) were prepared and characterized, using different techniques. Bonelike® analysis revealed the presence of hydroxyapatite, β-tricalcium phosphate (β-TCP) and α-tricalcium phosphate (α-TCP phases), resulted from the hydroxyapatite matrix reaction with glass, during the liquid phase sintering process.

Subsequently, a virtual 3D structure model was created and a CNC milling device machined the Bonelike® structure. The resulting structures showed a controlled macroporosity and interconnective structure. Macropores size after sintering was approximately 2000 μm.

The *in vitro* biological studies were performed using human bone marrow cells, which contains cells with the capacity to differentiate into bone cells. Cells were able to adhere and proliferate on 3D structures surface and migrate into all macropores channels. In addition, these cells were able to differentiate, since mineralized globular structures associated with cell were identified.

The results obtained showed that 3D structures of Bonelike® prepared by 3D machining with interconnected porosity and 2000 μm macropore size, allow with success cell migration into all macropores, as well as the bone marrow cells proliferation and differentiation.

Acknowledgements

I am grateful to my supervisors Professor José Domingos Santos and Dra. Anabela Dias for their helping hand and teachings.

My specials thanks to Professora Helena Fernandes for getting me started with cell work and constant support. I also would like to thank to all the members of Laboratório de Farmacologia da Faculdade de Medicina Dentária da Universidade do Porto, specially Dr. Pedro and Dra. Lurdes.

I whish to acknowlegement to everyone at INEB, especially the members of Laboratório de Biocerâmicos e Vidro. A special thanks to Eva Frias, David Cruz, Carlos Gonçalves and Sr. Ramiro for helping me with the isostatic press in the laboratory.

I would like to thank my family for the encouragement and support given during these two years.

Contents

List of figures and tables

CHAPTER 1
GENERAL INTRODUCTION

CHAPTER 1

1. The Bone

Bone is a specialized connective tissue that forms the skeleton of most vertebrates. It has the functions to support and protect the internal organs and provide attachment for muscles, facilitating the locomotion process [1, 2]. Moreover, it offers protection for blood-forming marrow and it is considered as a reservoir of mineral ions such as calcium, phosphate and other inorganic ions [3, 4].

1.1. Bone Composition

About 20%-30% (by weight) of cortical bone is organic, 10% is water and the remainder is mineral [1]. Bone is constituted by bone cells and an extracellular matrix, which has a mineral and an organic part.

Five main different cells can be found, like osteoblasts, osteocytes, osteoclasts, lining cells and osteoprogenitor cells, which will be described below [2,5].

The extracellular matrix is a physical support for cells, where they can adhere and interact. [3] The organic part of this matrix consists of collagen fibres, predominantly collagen I, the other components are various noncollagenous proteins such as: *osteonectin*, *osteocalcin*, *osteopontin*, *bone sialoprotein*, *proteoglycans* (decorin, biglycan), *glycoproteins* (thrombospondin, fibronectin, fibrillin), *enzymes* (alkaline phosphate, collagenase), and *cytokines* [6, 7]. Type I collagen provides a backbone for the deposition of bone mineral. The bone mineral crystals are aligned with their long axis parallel to the collagen axis [7]. Collagen fibres are responsible for bone elasticity, flexibility and the organization of the matrix [8].

Calcium and phosphate are the main components of the mineral part. Carbonate, citrate, sodium, magnesium, fluoride, hydroxyl, potassium and other ions can be found but in smaller amounts. The major mineral phase of bone is hydroxyapatite ($Ca_{10}(PO_4)_6(OH)_2$) (HA) [3, 9]. This apatite mineral is similar in composition and structure to minerals within the apatite group, which form naturally in the Earth's crust

[9, 10]. Collagen and HA are associated and assembled into a microfibrilar composite [11]. These crystals of HA give bone enough biomechanical strength [12]

1.2. Bone Structure

The adult long bones, anatomically, present a tubular shaft denominated as *diaphysis*. In the center of this section, is localized the *medullary cavity*, filled in with marrow (Figure 1). *Epiphysis* is found at each end of the bone. Separating these main parts is the *metaphysis* [2]. A fibrous membrane, *periousteum*, covers bone external surface (Figure 1). It is composed of dense connective tissue, presenting blood vessels. The medullary cavity, Havers and Volkmanm channels, and the cavities of cancellous bone are lined with a thin membrane, *endosteum* [13].

Bone marrow is divided in yellow and red marrow. The first one, is constituted, mainly, by adipose tissue. Red bone marrow fills the cancellous epiphysis of long bones. Large amounts of red bone marrow can also be found in flat bones like those of the ribs, iliac and skull [2, 14].

In bone marrow occurs the hematopoiesis. So, post-natal bone marrow is composed of a hematopoietic tissue and a stromal system [2, 15, 16]. Bone marrow stroma contain several type of cells that support hematopoiesis, including the mesenchymal stem cells [16].

Mesenchymal stem cells have the capacity of self-renewal and differentiation into several connective tissue lineages. They can give rise to osteoblasts, chondrocytes, adipocytes, tenocytes, hematopoietic-supporting stroma and nonmesenchymal cells, such as neural cells [17].

In addition, two different mature bone structures can be identify (morphologically or histologically) in different parts of the bone: compact (dense) and cancellous (trabecular) bone (Figure 2). Both exist in different proportion in several locations of the skeleton. Cortical or compact bone is highly dense and it is located on the exterior of the bone immediately underneath the *periosteum*. This type of bone is organized in cylindrical units, *Haversian systems* or *osteons*, and forms *diaphysis* of long bones.

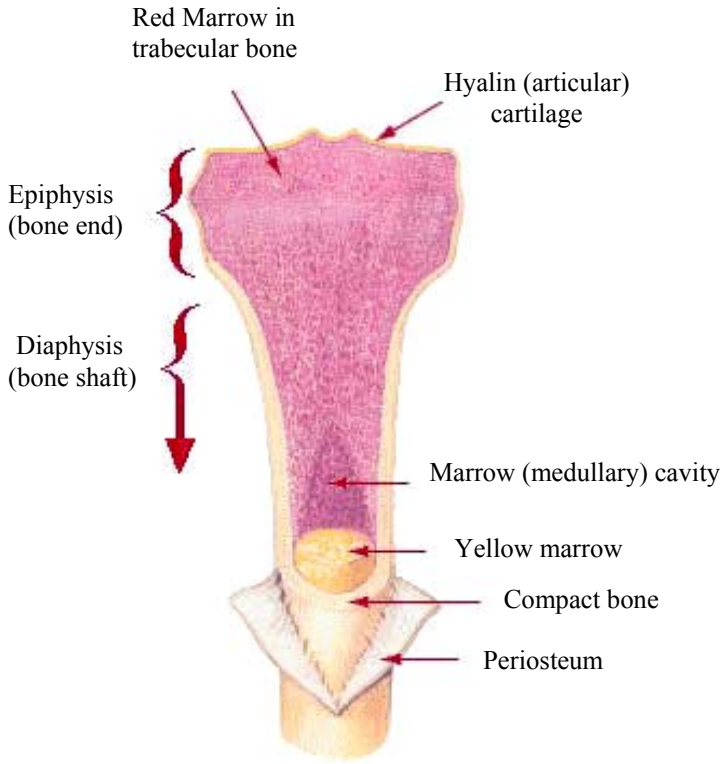

Figure 1 – Long bone anatomy [18].

Concentric layers called *lamellae*, composed by mineralized collagen fibres, constitute osteons. *Lamellae* are arranged in concentric rings around *Haversian canal* which has blood vessels, nerves and lymphatic vessels. Bone tissue has intercommunicating pores systems constituted by *canaliculi* (small canals), *lacunae* (spaces) and *Volksmann`s* canals which connect with *Harversian canals*. This bone is not remodelled so often as trabecular bone [1, 2, 13].

Trabecular or cancellous bone is porous and sited in the interior of bone. It is present in the *epiphysis* and has a *lacunar-canalicular* network to transport metabolic substances, as the compact bone. Nevertheless, this bone is organized in the form of thin interconnecting spicules and not in a *Haversian* system. Bone turnover occurs with great frequency [1, 2, 8, 13].

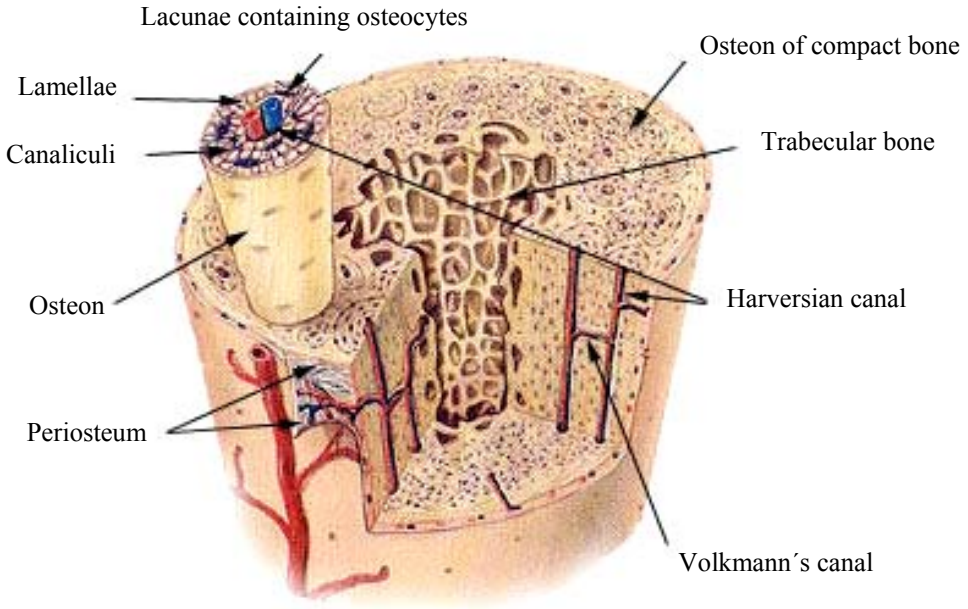

Figure 2 – Constitution of compact and cancellous bone [19].

1.3. Bone Cells

Five main different cells can be found in bone, such as osteoblasts, osteocytes, osteoclasts, lining cells and osteoprogenitor cells [2].

Osteoblasts

The first ones are mononuclear cells and their function is to synthesize the organic matrix and participate in mineralization of osteoid (unmineralized ground substance). An osteoblast has a prominent Golgi apparatus, typical of a protein-producing cell. So, they secrete collagen type I and noncollagenous proteins of the matrix [5, 6].

Osteoblasts are derived from mesenchymal stem cells. According to morphological studies, osteoblastic cells are categorized in a presumed linear sequence progressing from osteoprogenitors to pre-osteoblasts to osteoblasts and finally to osteocytes and lining cells [6, 20].

Factors such as bone morphogenetic proteins (BMPs) and transcription factors (Cbfa1) mediate and regulate the induction of mesenchymal stem cells into osteoblastic cells [20, 21].

When cells have committed to the osteoblastic lineage, they progress through three different developmental stages of differentiation: proliferation, matrix maturation, and mineralization (Figure 3). Genes are expressed during these stages and have been identified *in vitro*. In general, histone H4 and type I collagen peaks occur at proliferation stage. Alkaline phosphate peak occurs during matrix maturation, while osteopontin and osteocalcin peaks occur in the late matrix maturation or early mineralization phases [5, 6]

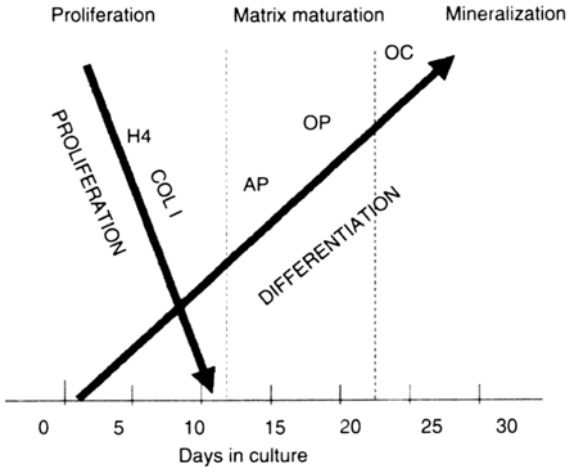

Figure 3 – The three principal periods of the osteoblast development in culture and the temporal expression of genes characteristic of this process. H4, histone; COL I, collagen; OP, osteopontin; AP, Alkaline phosphate and OC, osteocalcin [6].

Osteocytes

During matrix deposition, osteoblasts can be trapped in osteoid. They became osteocytes, surrounded by bone matrix or osteoid [2]. Osteocytes are in *lacunaes* and communicate with each other, and with blood vessels, throught minuscule canals, *canaliculi*, filled with cytoplasmatic projections. They are responsible for the

maintenance of bone matrix (synthesize and resorb matrix to limited extent) and the rapid release of calcium and phosphorous from mineralized bone into the blood [1, 2, 5].

Osteoclasts

Osteoclasts are responsible for bone resorption. They are multinucleated cells, originated from hematopoetic tissue with common differentiation pathways with macrophages [22].

Osteoclasts have multiple circumnuclear Golgi stacks, abundant lysosomal vesicles and a high density of mitochondria. Bone degradation begins when these cells attach a region of the matrix and dissolve bone [4].

Bone lining cells

Bone lining cells are present on bone surfaces where is not occurring bone formation or resorption. They are flat, elongated, relatively and only a few cytoplasmic organelles can be found [4]. Their function is to cover and protect bone surface. These cells and osteoblasts are originated from osteoprogenitor cells [8].

Osteoprogenitor cells

This type of cells can be found in the deepest layer of the periosteum, in the endosteum and bone marrow [3,16].They are recruited to repair bone defects, undergone differentiation.[3]

1.4. Bone Formation and remodelling

The ossification of skeleton occurs by two primary process: intramembranous and endrochondral. Intramembranous ossification occurs, predominantly in the cranial facial bones and parts of mandible and clavicle, where mesenchymal cells condense and

differentiate directly into osteoblasts. In most of other bones in the skeleton, enchondral bone ossification occurs, whereby mesenchymal cells condense to form a cartilage matrix [1, 5]. Upon vascular invasion of the cartilage template, the chondrocytes are removed and replaced by osteoblasts and osteoclasts. While the osteoclasts degrade cartilage, osteoclasts produce a bone specific matrix [1, 20].

Bone remodelling is the dynamic physiologic process by which bone mass is maintained constant throughout adult life in vertebrates. Bone remodelling consists of two phases: bone resorption by osteoclasts followed by bone formation by osteoblasts, and it occurs continually and simultaneously at multiple locations in the skeleton [20].

Bone resorption begins when osteoclasts attach to a site on the bone surface and remove bone by acidification and proteolytic digestion [7], creating a resorption pit. Sequentially, osteoblasts move in and fill the pit with organic matrix, which will be mineralized later. This process allows mineral ion homeostasis and it is regulated by various hormones, like parathyroid hormone, calcitonin, vitamin D, and estrogen [8]. Bone remodelling occurs due to the successive cycles of removal and replacement [4, 20].

1.5. Bone Healing

The bone fracture or the implant placement result in the loss of continuity of bone tissue at the site of injury and it is associated to the damage of the surrounding tissues. In both cases, the healing is a complex process that involves a multiple of cellular and extracellular events [21, 23].

Bone healing can be influenced by several factors like the bone type (cortical or trabecular), location and severity of trauma, species and age. Nevertheless, the outcome of successful healing is the reconstruction of tissue continuity [21].

In each case (fracture or implant) ligaments, muscles or blood vessel are damaged. The last one results in hemorrhage. Hemorrhage caused by the fracture or implant procedure results in the activation of the coagulation cascade and the final formation of a blood clot or hematoma. [21, 23] After hematoma, follows an acute inflammatory response. Inflammatory cells (macrophages, monocytes, lymphocytes,

and polymorphonuclear cells), fibroblasts and endothelial cells infiltrate the bone. Necrotic tissue and foreign bodies are removed by leukocytes. Next steps are the deposition and formation of granulation tissue, angiogenesis, and migration of osteogenic population (Figure 4) [21, 23, 24]. These cells are going to proliferate and differentiate, invading the bone chamber, or spread over the surface of bone (or implant)[21, 25]. At a final stage, the bone is restored to its original shape, structure, and mechanical strength. Much of the normal healing process is driven by growth factors and cytokines [23, 24].

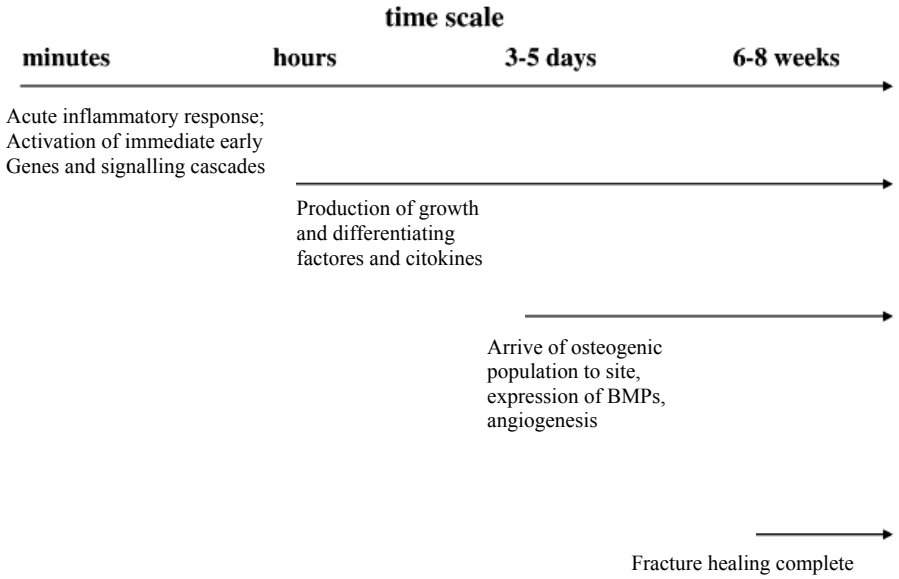

Figure 4 - Biochemical response to bone fracture [23].

1.6. Bone grafts

Medical problems can emerge from bone trauma, diseases and ageing. In order to solve these problems, autografts (autogenous bone), allografts (from human donnors) and xenografts (animal bone) have been used in bone surgery [26, 27].

Autografts is a tissue which is transplanted from one site, called donor site, to another called recipient site, on the same patient [28]. They are chosen due to their biological and physicochemical properties [29]. Cancellous and cortical bone, are usually implanted fresh, providing a source of osteoprogenitor cells and being

osteoinductive, osteocondutive and osteogenic. Nevertheless, these bone implantations show several limitations such as limited availability [29, 30], high post-operative pain and morbidity at the implant site [26].

Allografs are tissue transplanted from another member of the same specie [28] But it have also disadvantages such as the risk of viral transmission (HIV, Hepatitis), limited donor bone supply and requirement for immunosuppressant drugs [29, 30].

Xenografts are tissue transplanted from another specie donor. They can give rise to unfavourable immune response and viral or prion contamination. Due to these aspects, synthetic biomaterials have been developed [6, 28-30]. In summary, bone-derived grafts still have several limitations, and new synthetic materials have been developed and applied in Medicine. These materials can be an alternative to the use of autografts, allografts or xenografts for tissue reconstruction and regeneration.

2. Bone Tissue Engineering

Man-made materials have been developed to interface living host tissue, called biomaterials. These biomaterials used as bone grafts, are an alternative bone-derived graft avoiding the problems related to this kind of solutions. They have the advantages of availability, reproducibility and reliability [30].

In this context, occurs the development of a emerging field of science called Tissue Engineering (TE), which can be defined as "*an interdisciplinary field of research that applies the principles of engineering and the life sciences towards the development of biological substitutes that restore, maintain, or improve tissue function*" by Langer and Vacanti [31].

Tissue engineering uses three-dimensional scaffolds that help in the repair of the missing or damaged bone tissue, providing temporary 3D matrix for new tissue formation, [6, 31] recruiting surrounding host cells. They can also, deliver cells or bioactive factors to the bone defect site [31]. Scaffolds of different materials and architectures were created in order to promote a better and faster bone replacement. So,

scaffolds for use in bone tissue engineering must have several characteristics/requirements such as:

- Compatibility with human body, which means this must not elicit an unresolved inflammatory response nor demonstrate extreme immunogenicity or cytoxicity. This requirement is applied to the intact material and for degradation products [32].
- Biodegradability and bioresorbability with controllable degradation and resorption rates similar to tissue replacement; [31, 32-34]
- Osteoconductivity, osteoinductivity and osteogenecity [31].
- Adequate surface properties (chemistry, topography and surface energy)[35]; Surface chemistry and topography must be proper for cell distribution, attachment, proliferation, and differentiation; The ability of cells to adhere to the materials and the protein interactions are closed related with these properties[33, 34, 36].
- Three-dimensional (3D) structure with interconnected porosity to allow cell migration, tissue ingrowth, vascularization, flow transport of nutrients and metabolic waste [32, 33].
- Adequate mechanical properties [35]. Scaffolds must resist to the physical and chemical stresses of the host body, maintaining the structural integrity and the internal architectural stability [33].
- Adequate anatomical fitting [33], the shape and size must be adequate to the implant site [37].

2.1. Biomaterials

Biomaterials can be polymers, metals, ceramics, natural materials and composite materials (at least two different types of materials combined together) [3]. Although, the most common biomaterials used in bone tissue engineering scaffolds are polymers, bioceramics and composites, due to the controlled biodegradability [32, 38, 39].

2.1.1. Bioceramics

Ceramics are defined as inorganic, non-metallic materials which consist of metallic and non-metallic elements bonded together primarily by ionic and/or covalent bonds [40]. This type of materials has been used by humans for centuries. Although, more recently, they have been used to improve our quality life, helping in the repair and reconstruction of damage parts of the body (implants, prostheses, prosthetic devices).

All the bioceramics when are implanted in the body elicit a response of the host tissue, and both can suffer physical and/ chemical modification [28]. So, bioceramics can be divided in three different types based on different attachments and interactions between the implant and the tissue.

Bioinerts (or nearly inert) are bioceramics that are stable, almost biological inactive [41, 42]. These kinds of implants give rise to the formation of a non-adherent fibrous capsule at their interface. For example, Al_2O_3 or ZrO_2 fit in this class of bioceramics, developing a morphological fixation with tissue. Interfacial movements can occur and the implants may become loosen quickly [41].

Biodegradable or resorbable materials degrade gradually with time and are replaced by natural tissues. These are the ideal bioceramics, because they stay inside the body just the necessary time to the regeneration of tissue. [41-43]. However, the resorption rates must be similar to the repair rates of body tissues. In addition, they have to give mechanical support (strength and stability) in the early stages of bone healing. Later, the load will be transferred to the new replacement tissue. [32, 41] The degradation can be due to: the solubility of the material and local pH (physicochemical dissolution); fragmentation into small particles; and biological factors (biological dissolution) [28]. Successful examples of this kind of materials are β- tricalcium phosphate (β-TCP) and some bioactive glasses [41, 44].

Some bioceramics present *bioactivity* which may be defined as the "*ability to elicit a specific biological response that results in the formation of bond between the tissues and material"* [3]. They are called *bioactive ceramics* and include HA, some composites such as polyethylene-HA, some glasses and glass-ceramics. All the bioactive implants form a hydroxyl-carbonate apatite layer on their surface in simulated

physiological solutions. This layer is similar in composition and structure to the mineral phase of bone. The interfaces between bone and tendons and ligaments are quite similar to the interface between bioactive implant and bone. [41-44]

2.1.2. Hydroxyapatite

Calcium phosphate ceramics have been applied to repair damage parts of bone tissue. Different phases of calcium phosphate can be used for medical application, but hydroxyapatite (Ca_{10} $(PO_4)_6(OH)_2$) (HA) (Figure 5), has been widely used due to its bioactivity and to its crystallographic similarity to bone and dental tissues[8,45,46]. It belongs to the apatite group of minerals and its Ca/P ratio is 1.67. HA crystallizes into hexagonal system and has the unit-cell dimensions a = b =9.418Å and c= 6.884Å [10, 47].

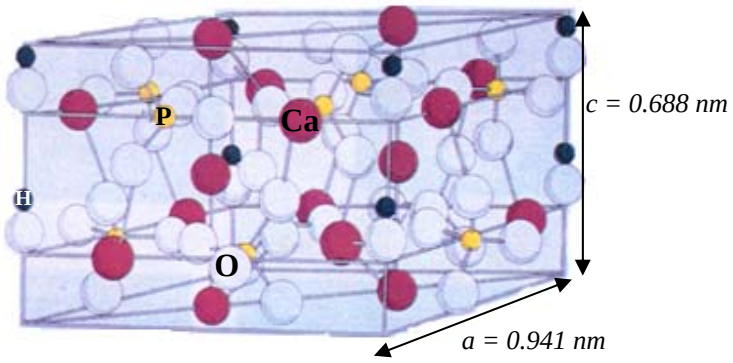

Figure 5 – HA structure [10].

2.1.3. Substituted apatites

Minerals are characterized by a unique combination of compositional and structural parameters. Nevertheless, the exact composition and structure of a mineral are somewhat flexible because they allow chemical substitutions. Comparing to the most other minerals, apatite is more flexible. These chemical substitutions slightly change the

structure of a mineral and often have effects on mineral properties, such as solubility, crystallinity, hardness, brittleness, strain, thermal stability, and optical properties (for example birefringence)[9].

In the same way, many ionic substitutions can occur in the apatite lattice changing the lattice parameters, morphology and are also critical to its crystallite size and dissolution rate [9, 42]. Chemical substitutions take place in the positions of the ions Ca^{2+}, PO_4^{3-} groups and OH^- groups. For example, the F^- can substitute OH^- causing an contraction in a-axis, which results in the increase of the crystallinity and stability. As consequence, flourapatite is less soluble then HA. On the other hand, carbonate CO_3^{2-} group, can substitute either hydroxyl OH^- or the phosphate group PO_4^{3-} [41-43]. The first type of substitution results in the contraction of c-axis, and the second type of substitution results in the opposite [42].

Biological apatites (human enamel, dentin, bone and some pathological calcification) are different from pure HA in some characteristics, such as stoichiometry, composition, crystallinity and other physical and mechanical properties. These apatites frequently are calcium-deficient and always carbonate substituted. In a general way, carbonate CO_3^{2-} groups can substitute phosphate group PO_4^{3-} and Ca^{2+} is substituted for Na^+ to balance charges. Small contents of other ions such as K^+, Mg^{2+}, F^- , Cl^- can also be found in this kind of apatites [8,41,42,48].

2.1.4. Other calcium phosphates

Calcium phosphates can be classified by their Ca/P ratios. In general, different Ca/P from 2.0 to 0.5 can be synthesized mixing calcium and phosphate ion solution under acid or alkaline conditions (Table 1) [3]. Related calcium phosphate phases can also be used as bone grafts, like tricalcium phosphate ($Ca_3(PO_4)_2$)(TCP). Two forms of TCP exists, α-$Ca_3(PO_4)_2$ (α-TCP) and β-$Ca_3(PO_4)_2$ (β-TCP) [3,47]. The dissolution rate of the several calcium phosphates is different depending of their Ca/P ratio. The extent of dissolution decreases following the order: α-TCP >β-TCP >HA [3, 81].

Table 1- Calcium Phosphates ceramics with their calcium phosphate ratios [3].

Ca:P	Mineral Name	Formula	Chemical name
1.0	Monetite	$CaHPO_4$	Dicalcium phosphate (DCP)
1.0	Brushite	$CaHPO_4.2H_2O$	Dicalcium phosphate Dihydrate(DCPD)
1.33	_____	$Ca_8(HPO_4)_2(PO_4)_4.5H_2O$	Octocalcium phosphate (OCP)
1.43	Whitlockite	$Ca_{10}(HPO_4)(PO_4)_6$	
1.5	_____	$Ca_3(PO_4)_2$	Tricalcium phosphate (TCP)
1.67	Hydroxyapatite	$Ca_{10}(PO_4)_6(OH)_2$	
2.0		$Ca_4P_2O_9$	Tetracalcium phosphate

2.1.5. Glass reinforced HA (Bonelike®)

In order to develop more effective scaffolds new composite materials emerge, as Bonelike®, where HA is reforced with $CaO\text{-}P_2O_5$ glass, prepared by a liquid-phase sintering route [49]. Ions from glass are involved in ionic substitutions that can occur in HA lattice, when the liquid glassy phase reacts with HA [50-52]. Consequently, this new material has a composition more similar to inorganic mineral part of bone, showing a higher bioactivity when compared to single phase HA [50,53,54].

The incorporation of glass incite the decomposition of the HA part to a secondary phase, β-TCP. Successively, at higher firing temperatures this phase change to α-TCP [50]. These secondary phases, improved the mechanical properties of Bonelike® [49, 53, 55] and are known to have a higher dissolution rate than HA. Due to this, Bonelike® can be used in medical applications which require higher degree of dissolution and faster healing process [52, 54-56].

The secondary crystalline phases that can occur in Bonelike® are dependent of the content of glass, composition added and the sintering conditions [54].

2.1.6. Medical applications

Calcium phosphate-based bone grafts have been used in hard tissue surgery [53] such as craniofacial, oral/maxillofacial, orthopaedic and dental surgery [3, 10, 28]. The bioceramics used, can have different forms (granules, porous or dense bodies and cements) and shapes (for example spherical, polyhedral, platelike) depending on the surgical application [10, 28]. For example, granules can be used to fill bone defects or voids of tumours or cysts. Polyhedral blocks can be used to support long bone fractures or in spine union cases [10, 54].

2.2. Porous bioceramics

Porous bioceramics in general, promote the ingrowth of tissues into pores (biological fixation), providing a large interfacial area between tissue and the implant, due to their surface porosity. The idea of this kind of materials is to prevent loosing of implants, improving mechanical fixation of the material in the implant site [41, 58, 59].

Porous sizes that can be found in normal bone are in the range of 1-100μm. Small porosities like *canaliculi* or smaller *lacunae* size is between 1 to 5μm. On the other hand, osteocytes *lacunae* and Volksmann`s canals have 5-15 μm and the larger ones Haversian canals, present diameters between 50-100 μm [60]. Therefore, pores size larger than 100μm is necessary for cell migration and attachment and for capillaries provide blood and nutrition to the ingrown tissue [41, 60]. Pores must also be interconnected to allow cell migration, circulation of water, nutrients, gases [61] and the removal of metabolic waste [58].

Porous bioceramics can be prepared from different ways for biomedical applications, like conversion from natural structures and completely synthetic techniques [59, 61-64]. The first ones start with a natural porous structure, like a coral [65, 66] or trabecular bone [67, 68], which is converted to the final composition, maintaining the original structure [59]. Other conventional methods, completely synthetic, had been used for creating porous, such as foaming techniques (foams and

sponges) [69, 70] and introduction of porogenous substances (organic additives, salts) [71, 72].

In a general way, foaming techniques use polymeric foams or sponges. They are mixed with the material (for example HA slurry). After that, the mixture is dried and is heated up to a convenient temperature, in order to burn-out the foam or sponge. These techniques allow the fabrication of HA with an open-pore structure [69, 70, 73].

In the other technique, different porogenous substances like organics additives [64] (for example potato starch, organic polymers, almond crust) or salts (sodium chloride NaCl) can be mixed with ceramic material, leaving a macroporous structure after the right treatment [52, 74].

The substances used in some of these methods can leave residues. These particles may damage cells and nearby tissues [75]. Another problem of conventional methods is the uncontrolled porosity and shape generated (Figure 6a) [76]. In this thesis, it was decided to use techniques that allow fully control of the porosity (pore size, pore shape, pore distribution, pore interconnectivity and density) [37, 58] and avoid the impurities. Furthermore, scaffolds should have a defined architecture with right shape to a specific implant site. All these requirements can be accomplished using 3D Biomodelling techniques Rapid prototyping (RP) and 3D machining.

Figure 6 – Uncontrolled porosity produced by a conventional technique (a) [74] versus controlled porosity produced by rapid prototyping (virtual image) (b) [77].

2.3. 3D Biomodelling

In this thesis is proposed a revolutionary way for the development of new scaffolds using 3D Biomodelling. Biomodelling is a term used to describe "*the ability to replicate the morphology of a biological structure in a solid substance*". The morphological data is processed by a computer which generate a code necessary to construct a physical model, through prototyping techniques [78]. Morphological and anatomical data from patients can be captured using radiant energy (3D medical imaging scan). As result, the 3D physical models can show particular anatomical sites with great complexity due to trauma, ageing and tumor diseases, enhance the medical diagnosis quality. These models can be very helpful for surgical planning or act as an aid during surgery, diminishing surgical risks for patients [31, 78, 79]. 3D scaffolds can also be designed and manufactured according to the morphology of the tissue, size and conformation of the implant site. In summary, 3D Biomodelling can give the correct anatomic design, contour, biofunctionality and morphology (macro-microporosity) of the bone defect areas allowing the construction of adequated scaffolds, prostheses and 3D physical models [80].

2.3.1. Prototyping techniques

The more current traditional technologies to manufacture archetypes in the most diverse materials are: manual modelling, build maquettes, carpentry of moulds and conventional computer numerically controlled (CNC) machining [81]. More recently, about 12 years ago, emerge rapid prototyping (RP) [82, 83].

CNC machining can be used to construct 3D scaffolds. It consists of the removal of material, from an initial block, until getting the final desired form [81].

Numerical control (NC) is the method of giving instructions to a manufacturing machine based on a code of letters, numbers, and special characters [84, 85]. The machine responds to a program (complete set of coded information for executing an operation) which is translated into corresponding electrical signal for input to motors that run the machine [84]. The instructions can be the positioning of the machine

spindle relative to the workpiece (movement along axis directions) or controlling the speed and direction of spindle [85]. A CNC machine is an NC machine with the added feature of an on-board computer [84].

Rapid Prototyping (RP) includes several technologies that are able, from 3D computer data sets, to produce 3D physical models [58, 59, 77]. Some of these fabrication techniques have been used for medical applications, such as Stereolitography (SLA), Selective Laser Sintering (SLS), Fused Deposition Modeling (FDM) and 3D Printing, where the physical structures are build through a layer-by-layer additive process [34, 58, 87].

A computer, through adequate software, designed the macroporosity of the scaffold developed in this work, and a CNC milling machine constructed scaffold through a material removal process. The aim is designing a porous calcium-phosphate ceramic with accessibility for bone forming cells.

3. General aspects of Cell cultures

3.1. Cell adhesion, proliferation and differentiation

In biomaterials domain, bone cell adhesion involves first the attachment phase where physico-chemical linkages between cells and materials (ionic forces, van der Walls forces, and so on) are established in a very quick time. Then, the adhesion phase occurs involving several biological molecules, like extracellular matrix proteins, cell membrane proteins and cytoskeleton proteins. The quality of this phase is going to influence the cell's capacity to proliferate and differentiate in contact with the material [88].

Cell proliferation is related with *cell cycle*, which is regulated by signals of the environment. Through this cycle of duplication and division, genetic information is copied and passed to the next generation of cells [89]. The animal cell cycle is divided in four phases: Interphase which includes G_1, S, G2 phases and M-mitosis phase (Figure 7).

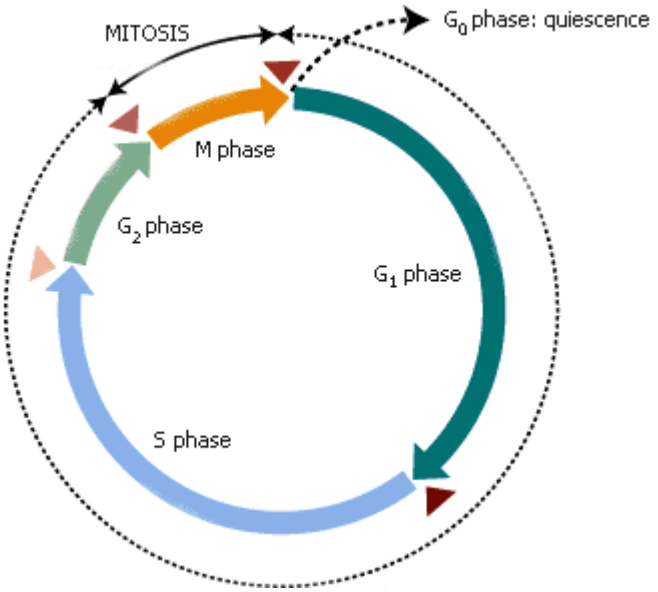

Figure 7 - Cell cycle divided in G_1, S, G2, M-mitosis, G_0 phases [90].

During all interphase, cell transcribes genes, synthesizes proteins and grows in mass. The S phase is characterized by nuclear DNA replication. $G_1$and G_2 phases provide time to cells prepared themselves for initiate mitosis and duplicate their cytoplasmatic organelles. During the stage M - mitosis, the cell's chromosomes and the other cellular components are divided between the two daughter cells. Cells can enter in an extended G_1 (also called G_0 phase or state of quiescence) when temporarily or reversibly stopped dividing [89, 91].

Senescence occurs due to intrinsic factors that regulate the cycle such as p53 proteins and the inability of telomeres to replicate at each cell division. They become shorter until reach minimum length, and cells can no longer divide [92].

Differentiated cells have limited capacity to proliferate, so they normally do not contribute to the formation of the primary culture. The proliferating cells are in the origin of this culture. Giving the correct conditions, undifferentiated precursors may propagate and differentiate following the desired pathway (Figure 8). To promote the differentiation it is required high cell density, enhanced cell-cell interactions and cell-matrix interactions and the presence of several differentiation factors .This will require a

selective medium, supplemented with factors that favour differentiation, such as β-glycerophosphate and dexamethasone (Figure 8) [6, 92-94].

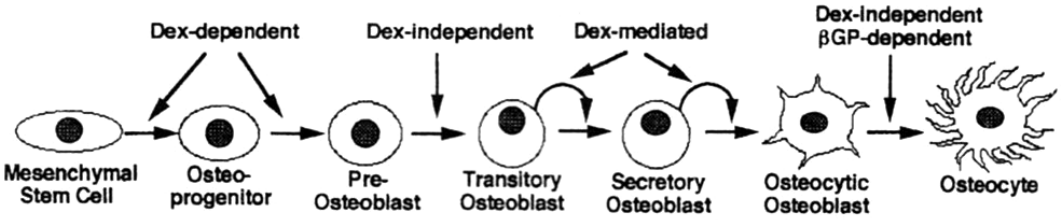

Figure 8 - *In vitro* Osteogenic induction of mesenchymal stem cells by dexamethasone (Dex) and β-glycerophosphate (βGP) [94].

3.2. Cell culture methods

Cells can be removed from original organs or tissues and placed into an artificial environment where can be maintained. Typically, a suitable glass or plastic vessel with a liquid or semi-solid medium characterizes the artificial environment. The medium provides necessary nutrients for survival and growth [95].

Two main methods are used to initiate a culture:

- A small fragment of tissue can adhere (*primary explant culture*) to a glass or plastic surface, promoting cell migration, also known as *outgrowth* [92, 93].

- Tissue sample can be disaggregated (mechanically or enzymatically). Consequently, normal relationships between cells is also disrupted [92, 95].With this last method larger cultures are obtained more rapidly when compared with explant culture. Although, explant culture present advantages when cells are very fragile or only small fragments of tissue are available [93]

Two basic systems can be used for growing cells: *monolayer culture system* or *suspension culture system*. In the first system, cells are cultured on a solid or semi-solid substrate, and the proportion of cells capable of attachment forms an adherent monolayer (*anchorage-dependent*). The cells capable of proliferation will be selected at the first subculture, and may give rise to a *cell line* [93, 95]. *Suspension culture* are used when cells can proliferate without attachment (*anchorage-independent*) like hematopoetic cells, cells from malignant tumours or transformed cell lines [92].

After the monolayer culture is establish *confluence* is reached when *all the available growth area is utilized and cells make close contact with one another*. High cell density can inhibit proliferation as well as change cell shape [93, 96]. To avoid this, *passages* can be made to keep a low cell density. To *subculture* a cell line, cells have, in first place, to be dissociated from the substrate and from each other, usually using trypsin, prontase, dispase or collagenase [93].

The majority of cell lines can be propagated in an unchanged way during a limited number of generations [96]. *Finite cell lines* undergo through limited passages, reaching senescence [92]. *Continuous cell lines* have the ability to grow continuously [93]. The transformation *in vitro* to this kind of cell line can occur spontaneously, or be induced by virus or chemical substances. These cells can also be obtained from tumour tissues [96].

Each time that a cell line is subcultured, immediately after seeding, cells enter in a latent period (*Lag period*). This period allow cells to recover from trypsinization, reconstruct the cytoskeleton, secrete matrix and spread out on the substrate. After that, cells enter in exponential growth (*log phase*) when cell population doubles. Cells occupied all the substrate and enter in the *plateau* (*stationary phase*), and the growth is much reduced. At this stage, several cells differentiate or enter in G_0 phase of cell cycle. The next subculture, ideally, should be carried out before reaching the plateau (Figure 9) [92].

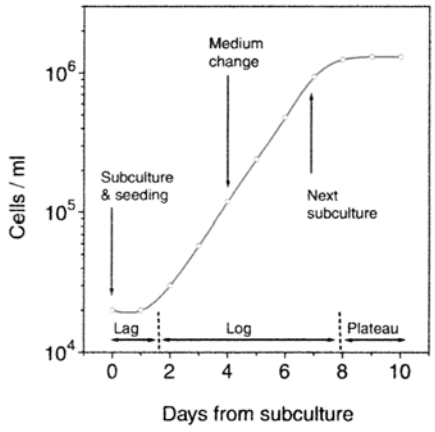

Figure 9 – Growth curve showing the lag, log and plateau phases [92].

3.3. Cell culture characterization

Cell culture characterization is usually based on the evaluation of several parameters characteristics of the cells in culture, such as cell adhesion and morphology, cell growth and functional activity. This characterization involves the use of different methods, which can be classified in two groups: qualitative and quantitative methods [97].

3.3.1. Qualitative methods

Qualitative methods include microscopy techniques, such as scanning electron microscopy (SEM) and confocal laser scanning microscopy (CLSM).

SEM gives images of samples surface with high resolution and depth of field [3]. Small structures can be identified on biological surfaces with this technique, such as nuclear pore complexes of cells and collagens [98] and it also allows for the identification of mineralised deposits characteristics of osteoblastic culture [96].

Confocal microscopy is very useful for the multidimensional analysis of biological samples. Its fundamental principle is to eliminate out-of-focus light, increasing micrograph contrast and/or reconstructing three-dimensional images.

Using these techniques it is possible to characterize cell morphology (shape and appearance), cell adhesion, 3D distribution of the cells, and evaluate cell viability on biomaterials [99].

3.3.2. Quantitative methods

The quantitative methods analyze the cell growth and supply information of the cell metabolism [97].

Cell growth or proliferation can be determinated based on cell quantification in the population. An electric counter can directly count the number of cells. Other techniques count some cell constituents, like total protein and DNA analysis [1, 97]. Methods that supply information about cell metabolism, such as MTT reduction can

also evaluate the cell's viability and proliferation [96, 97]. Functional parameters are evaluated by enzyme activity, characteristic of the cell type in study. In osteoblastic cultures, usually it is evaluated the alkaline phosphatase activity (ALP) and expression of bone matrix proteins (collagen type I; osteocalcin; fibronectin) [96].

CHAPTER 2
EXPERIMENTAL PROCEDURES

Chapter 2
Experimental procedures

Introduction

In the present chapter it is described the laboratorial procedures for: 1) the preparation and characterization of the hydroxyapatite and Bonelike® ; 2) the preparation and characterization of macroporous Bonelike® three-dimensional structures and 3) the *in vitro* biological studies.

The Bonelike® powders were prepared following the steps: preparation of the HA through a precipitation method, preparation of a P_2O_5-CaO based glass and mixture of glass with HA powders.

The physico-chemical and structural characterization of the bioceramics prepared were performed using the X-ray powder diffraction (XRD), Fourier transform infrared (FTIR) and Scanning Electron Microscopy (SEM) techniques.

The dense cylindrical Bonelike® samples, prepared by powder compactation, were machined through a CNC milling machine. This machine removed the material according to a virtual model, constructing a scaffold with the desired macroporosity and 3D structure.

3D macroporous samples density was evaluated by Archimedes´ Principle using a density determination kit of an electronic balance. 3D macroporous samples were measured, before and after sintering by a SEM and a Stereomicroscope.

The behaviour of bone marrow cells cultured on 3D macroporous Bonelike® samples was evaluated through Confocal Laser Scanning Microscopy (CLSM), SEM and Stereomicroscope techniques.

1. Preparation of Hydroxyapatite and Bonelike®

1.1 HA preparation method

HA was prepared through a precipitation method consisting of the reaction between calcium hydroxide $Ca(OH)_2$ and ortho-phosphoric acid $H_3(PO_4)_2$, following the reaction:

$$10\ Ca(OH)_2 + 6\ H_3(PO_4)_2 \rightarrow Ca_{10}(O_4)_6(OH)_2 + 18H_2O \qquad \text{(eq. 1)}$$

During the synthesis process, an aqueous solution containing $H_3(PO_4)_2$ was added to a suspension containing $Ca(OH)_2$ in distilled water, through a peristaltic bomb (Figure 10). The suspension was maintained in vigorous stirring.

The pH control of the solution was ensured by the addition of ammonia solution NH_3 (32%), keeping the pH values above 10.5.

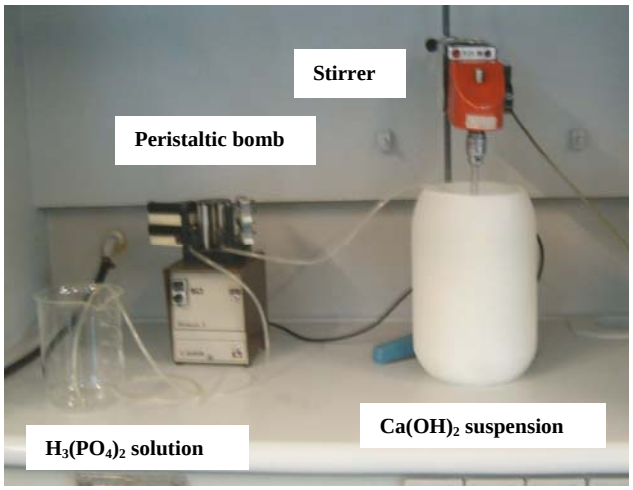

Figure 10- Chemical reaction apparatus of HA.

After 3 hours of stirring, the final HA solution was left ageing overnight. Then, the resulting precipitate was filtrated through a vacuum system, using paper filters without ashes to avoid HA contamination. The resulting batch was dried in an oven at 60ºC, for two days.

1.1.2. Milling and sieving

HA was crushed and milled in agate mortar to avoid contaminations. Then was stainless sieved under 75 μm (250,120 and 75 μm steel sieves) to destroy the agglomerates, using a Retch Vibratory Sieve Shaker.

1.2. Glass preparation method

A glass of the P_2O_5-CaO system (65 P_2O_5, 15CaO, 10CaF_2, 10Na_2O mol%) was prepared, starting by weight the appropriate quantities of high purity (>98%) grade reagents, sodium carbonate (Na_2CO_3), calcium hydrogenphosphate ($CaHPO_4$). calcium fluoride (CaF_2) and di-phophorous penta-oxide (P_2O_5). The reagents were mixed in a platinum crucible, and then heated at 1450ºC for 90 minutes in a furnace. After 2 hours, the molten glass was poured into a steel mould.

1.2.2. Milling and Sieving

Glass was crushed in agate mortar to avoid contaminations. Then, it was mixed with methanol and agate balls. The mixture was milled in a agate ball mill pot (Figure 11). After that, the glass was dried and sieved under 75 μm using a Retch Vibratory Sieve Shaker.

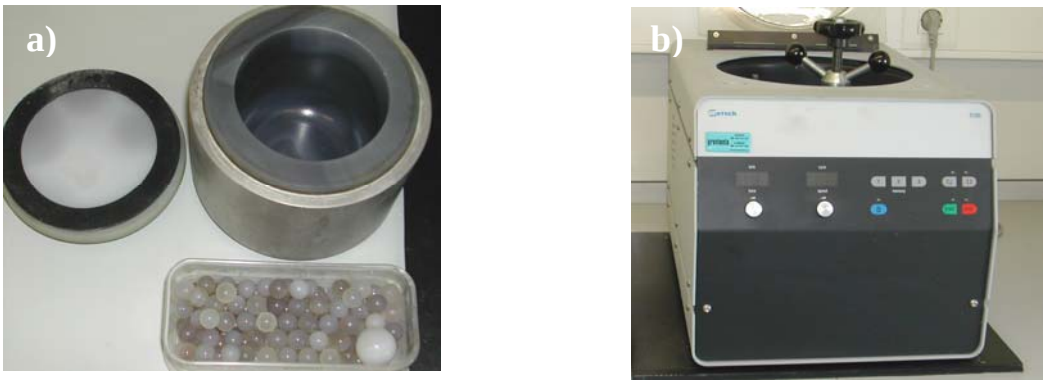

Figure 11 – (a) Agate balls and pot (b) rotative ball mill.

1.3. Bonelike® preparation method

Bonelike® was prepared by adding 2.5% of glass with the laboratory prepared HA in iso-propanol (as suspending medium). The powders were mixed for 6-8 hours. The wet homogeneous mixture was dried in a oven at 60ºC for two days and sieved under 75 μm, using a Fritsch Vibratory Sieve Shaker.

1.3.1 Pressing

To prepare the dense Bonelike® cylindrical samples of approximately 15.5 mm diameter and 7.3 mm thickness, the powder undergone two types of pressing, uniaxial and isostatic.

Firstly, the specimens were pressed using a uniaxial press (Figure 12). The cylindrical die (Figure 12) was filled with 2.5g of powder material to prepare each sample. The sample was pre-loaded to obtain a perfect alignment of the cylinder with the steel die. After that, the load was increased to 120 Bar.

a)

b)

Figure 12 – (a) Cylindrical die and (b) uniaxial press.

The next step was to press the samples at 1600 bar, using a cold isostatic press. The samples were involved in polyethylene bags. After pressing, the samples were dried overnight in a oven at 60ºC.

1.4. Sintering

HA and Bonelike® powders were sintered in a muffle furnace with a Eurotherm type 2408 controller. The samples were sintered at 1300ºC using a heating rate of 4ºC/min with 1hour dwelling time at 1300ºC, followed by natural cooling inside the furnace. Powders were placed on Alumina (Al_2O_3) plates to avoid contact with furnace floor.

Physico-chemical and structural characterization

X-ray powder diffraction (XRD)

After sintering, HA and Bonelike® samples were ground to fine powders and were analysed by a Rigaku Dmax-III-VC X-ray diffractometer, using CU-Kα radiation (Kα = 1.54056 Aº). Data were acquired from 4 to 80º 2θ, with step size of 0.02º/s.

Fourier transform infrared (FTIR)

The infrared spectra analysis was performed with a FTIR system 2000 from Perkin-Elmer, with and 4cm $^{-1}$ resolution and 100 scans. The HA and Bonelike® were ground to fine powders and sintered as referred in 3.4 and mixed with potassium bromide (KBr) (2mg of material with 200mg KBr). Thin discs were prepared using a steel die under uniaxial pressing. The molecular groups of a specific functional group have characteristic vibration frequencies, in well-defined areas of spectrum range [47].

Scanning electron microscopy (SEM)

SEM observations were performed with a JOEL JSM-6310F scanning electron microscope. The Bonelike® cylindrical sample was attached to carbon tape in an aluminium support. Finally, they were coated with gold about 13 minutes.

2. Preparation and characterization of 3D macroporous Bonelike® structures

3D machining

Cylindrical dense specimens of HA and dense Bonelike® were prepared as described in chapter 2, and placed into a metal support of a CNC milling machine Roland Modela desktop MDX 20 (Figure 13a). Previously, the support was attached to the flat working table of the machine and the milling head (figure 13b) was fitted on it. This milling head moved into a series of stepped movements along x, y, and z directions, according to the coded information sent by a computer. The machine start to perforating the dense samples in specific coordinates, according to the virtual model generated by the 3D CAM software (deskproto). One spindle of 2.5 mm diameter was used (Figure 13c).

The final structure presented seven macropores on both, top and bottom surfaces, and also six macropores all around lateral face. These cylindrical structures are represented in Figure 14. After machining, the samples were sintered as described in item 1.4.

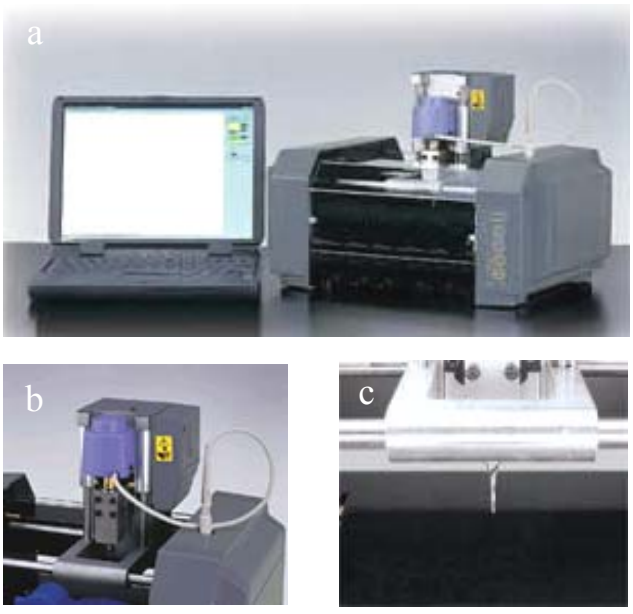

Figure 13– (a) CNC milling machine connected to a computer [100] with the milling head fitted (b) and with the rotative spindle (c) [101].

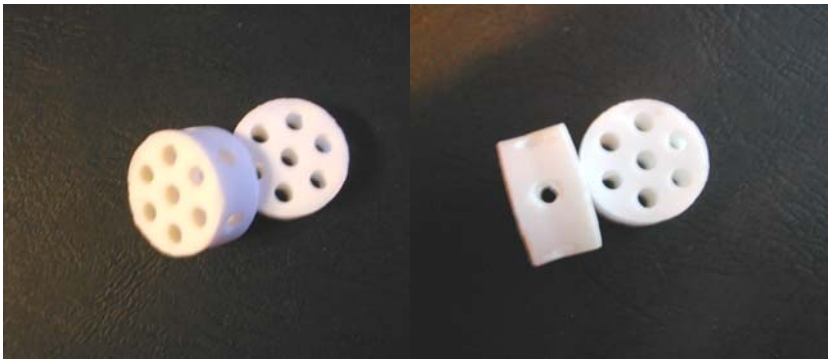

Figure 14 – Final macroporous structure.

Macroporous samples characterization

Samples density

The determination of 3D macroporous structures densities was performed on six sintered Bonelike® samples through a density determination kit of electronic Mettler Toledo balance. The density of the solid sample was calculated using the following equation (eq. 2):

$$\rho_2 = \left(\frac{A}{A - B} \right) \times \rho_0 \qquad \text{(eq. 2)}$$

Legend:

ρ_2 = Density of the sample

A = Weight of the sample in air

B = Weight of the sample when immersed in test liquid

ρ_0 = Density of test liquid at a given temperature t

Samples were submerged in deionised water and the density of water, ρ_{water}, was 0.9966 g/dm^3 at measured temperature of 26.5ºC.

Microscopy and image analysis

Scanning electron microscopy (SEM)

SEM observations were performed with a JOEL JSM-6310F scanning electron microscope. The cylindrical dense samples of HA and Bonelike® were not polished. Some samples were attached to a carbon tape in an aluminium support and others were laterally involved with araldite and attached to the aluminium support. Finally, all the samples were coated with gold for 13 minutes.

Stereomicroscope System

Macropore size (n=10), macropore distribution (distances between adjacent macropores) (n=10), sample diameter (n=6) and sample thickness (n=6), before and after sintering were measured by SEM and Stereomicroscope system Olympus SZX9. The images were acquired by a digital camera linked to the microscopy and treated with adequated software, in order to be possible to obtain the measurements referred to above.

3. *In vitro* biological studies

Cell culture

Human bone marrow and fragments of trabecular bone were collected during orthopaedic surgery procedures. To initiate the culture, trabecular bone sample was mechanically disaggregated and washed with standard culture medium, as result a single-cell suspension was obtained. To this suspension was added a bone marrow cells suspension. The cells were cultured in minimum essential medium Eagle, alpha modification (α-MEM) containing 10% foetal bovine serum (FBS), 100µg/ml penicillin, 10IU/ml streptomycin, 2.5 µg/ml fungizone and 50µg/ml ascorbic acid. Incubation was carried out in a humidified atmosphere of 95% air and 5% CO_2 at 37ºC. The passage was made when primary culture was near confluence. Adherent cells were enzymatically released (trypsin trypsin-EDTA solution) and counted using a

hemocytometer. Cells from the first passage were seeded on biomaterials at a density of 2 x 10^4 cells/cm^2 and cultured using the same experimental conditions, those used in the primary culture, with a different supplement medium (50μg/ml ascorbic acid, 10mM sodium β-glycerophosphate and 10 nM dexamathasone). The biomaterial samples were pre-incubated with this medium for 1 hour at 37ºC, in a humidified atmosphere of 95% air and 5% CO_2. Culture medium was changed twice a week. Cultured material samples were observed by CLSM, SEM and Stereomicroscope at days 3, 7, 14 and 28.

Confocal laser scanning microscope (CLSM)

Cells were fixed with 4% formaldehyde (methanol free), permeabilized with 0.1% triton and incubated in 10 mg/ml bovine serum albumin (BSA) with 100μg/ml RNAse. F-actin filaments were stained with Alexafluor-conjugated phalloidin and nuclei were counterstained with 10 μg/ml propidium iodide. Samples were washed with PBS and covered with Vectashield. Images were acquired on a Leica TCP SP2 AOBS.

Scanning electron microscopy (SEM)

Cells were fixed with 1.5% glutaraldehyde in 0.14 M sodium cacodylate. The samples were dehydrated in graded series of alcohols and critical point dried. Specimens were mounted onto aluminium supports using araldite and then sputter-coated with gold and observed in a Joel JSM 35C scanning electron microscope equipped with an X-ray energy dispersive spectroscopy voyager XRMA System, Noran Instruments.

Stereomicroscope

The same samples prepared for CLSM observations were used for Stereomicroscope. The Stereomicroscope Nikon SMZ 1500 was equipped with a fluorescence illuminator.

RESULTS

RESULTS

1. Characterization of Hydroxyapatite and Bonelike®

XRD analysis

XRD pattern of HA prepared shows that it is phase pure (Figure 15). Bonelike® XRD data set (figure 15) confirmed the presence of HA, α-TCP and β-TCP in the respective proportions 69%, 24% and 7%.

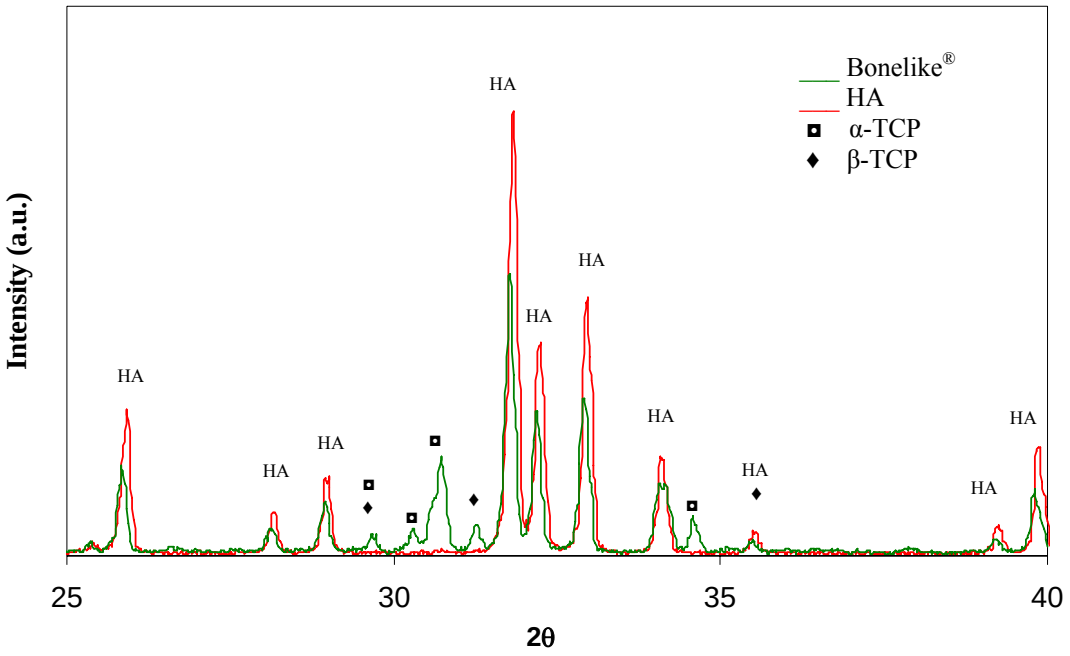

Figure 15 – Overlaid traces of Bonelike® and HA XRD data sets with all the present phases identified (HA, β-TCP and α-TCP).

Ftir analysis

Analysis of FTIR spectra of HA reveal the presence of the groups PO_4^{3-}, OH^- and H_2O. Hydroxyl OH^- peaks were detected at 3570 cm^{-1} and 630 cm^{-1}. The board band

observed at 3200-3600 cm^{-1} indicate adsorbed water on the materials. Phosphate peaks were detected at 566, 597, 958, 1041, and 1086 cm^{-1}. Bonelike® reveals the same peaks for the same groups. One peaks of hydroxyl (630 cm^{-1}) underwent a significant decrease in intensity (Figure 16).

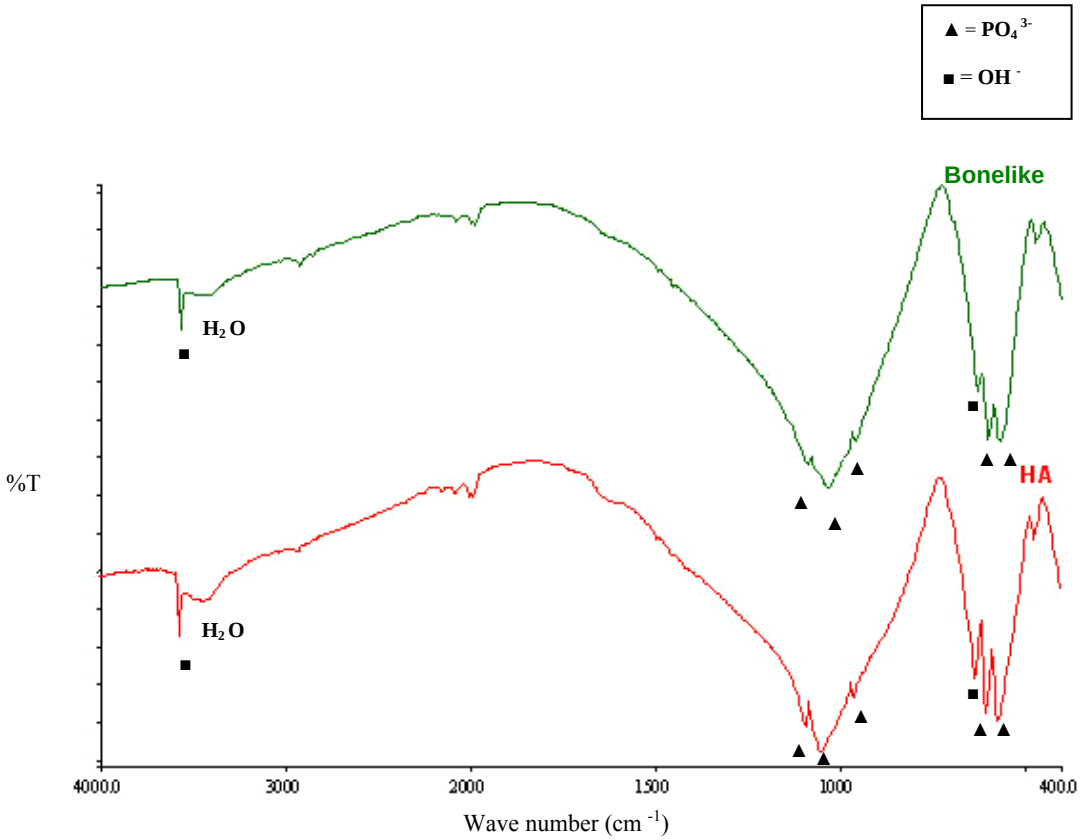

Figure 16 – Overlaid traces of Bonelike® and HA FTIR spectra with all the present groups identified (PO_4^{3-}, OH^- and H_2O).

SEM analysis

The results from SEM analysis are shown in Figures 17. Bonelike® present a rough sandblasted surface, with occasional cavities. Inside the Bonelike® cavities, pores seem to be connected forming a continuous network separated by walls of material, as referred to in literature [56].

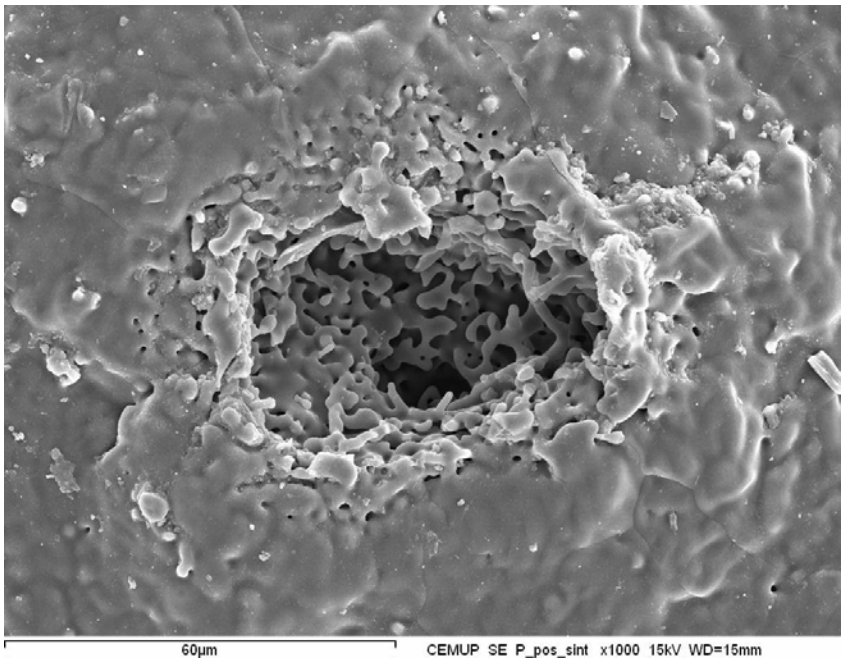

Figure 17 - SEM imagine of Bonelike® surface with a porous cavity.

2. Characterization of 3D macroporous Bonelike® structures

The average and standard deviations density of macroporous sintered Bonelike® samples are indicated in table 2.

Table 2 – Density of the macroporous Bonelike® samples.

Material samples	Density (g/cm^3)
Bonelike®	2.924 ± 0.073

The averages and standard deviations of the different measurements in porous samples, before and after sintering, are indicated in table 3. The percentage of densification calculated for the samples is approximately 95%.

Table 3 – Different measures of the macroporous samples before and after sintering (mm).

Bonelike®	Pore size	Distance between pores	Sample diameter	Sample thickness
Before sintering	2.696 ± 0.055	2.121 ± 0.066	15.539 ± 0.083	7.30 ± 0.201
After sintering	1.967 ± 0.062	1.962 ± 0.070	12.560 ± 0.090	5.84 ± 0.209

The samples maintained their original structure and cylindrical geometry after sintering (Figure 18). However, their dimensions decreased as confirmed in table 3. The percentage shrinkage of pore size was 27%; the distances between adjacent pores was 8% and the sample diameter was 19%. Most of the samples presented cracks all around the surface, next to sample border (Figure 19).

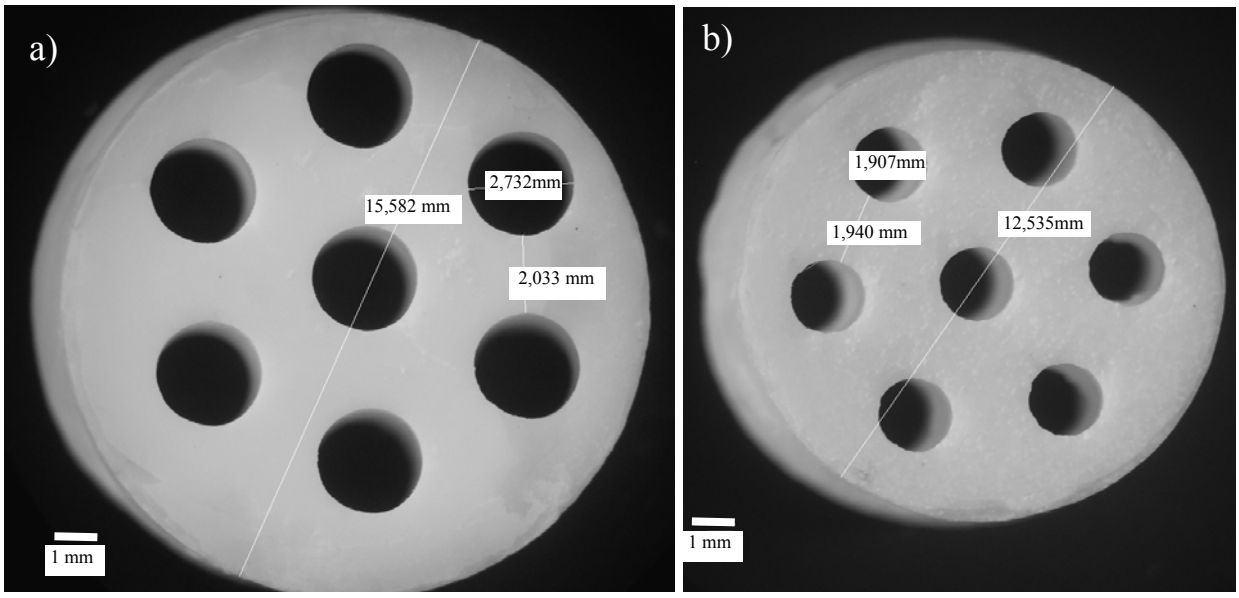

Figure 18 – Different measures of the macroporous samples before (a) and after sintering (b).

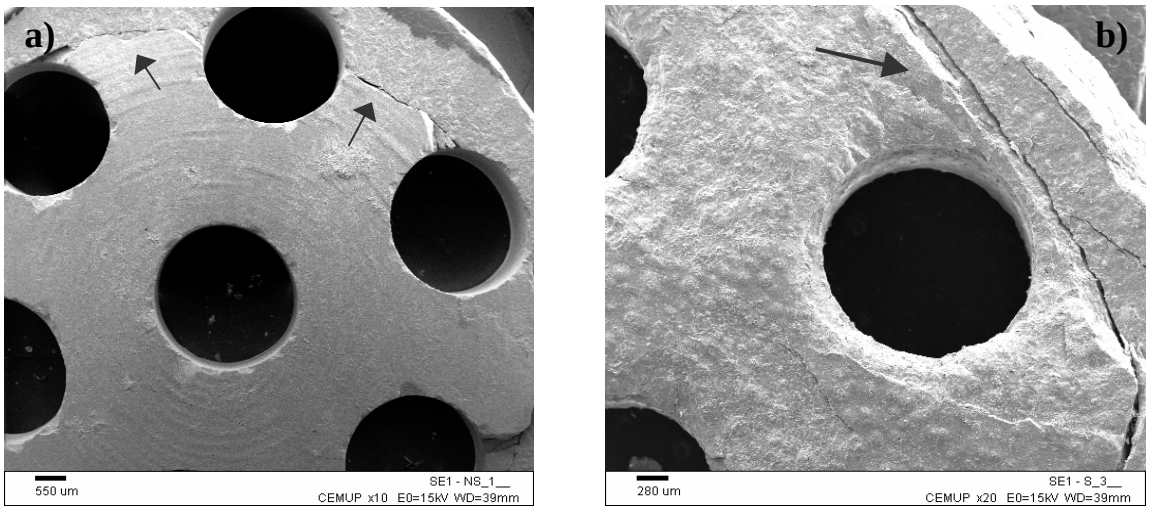

Figure 19- Cracks around the surface in (a) non-sintered and (b) sintered sample.

3. *In vitro* biological studies

The growth of bone marrow cells was observed and recorded. CLSM and Stereomicroscope images of cells after 3 days of culture on macroporous Bonelike® are presented in Figure 20. Cells were able to spread and covered the surface sample, starting to form a continuous cell layer and adopted a typical osteoblast-like morphology. Figure 20b shows that cells started the migration into macropores. The samples were broken to allow the observation of its interior. In Figure 20c is confirmed that a few cells were able to reach the internal surface of macropores, although in a lower density when compared with surface colonization.

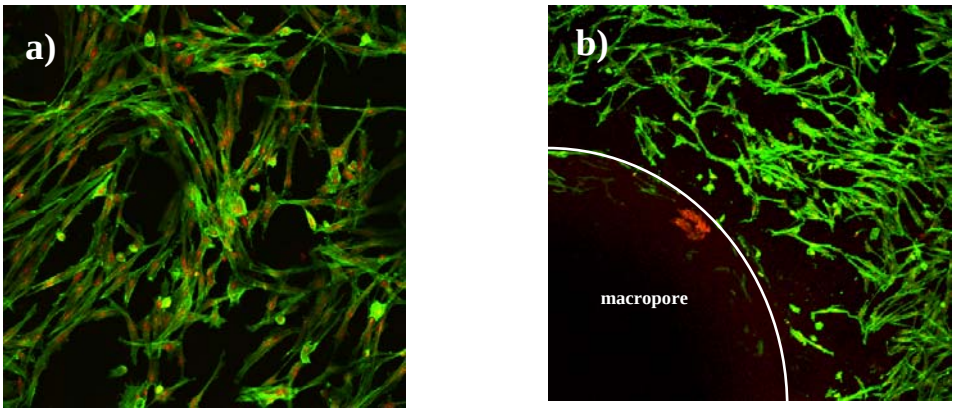

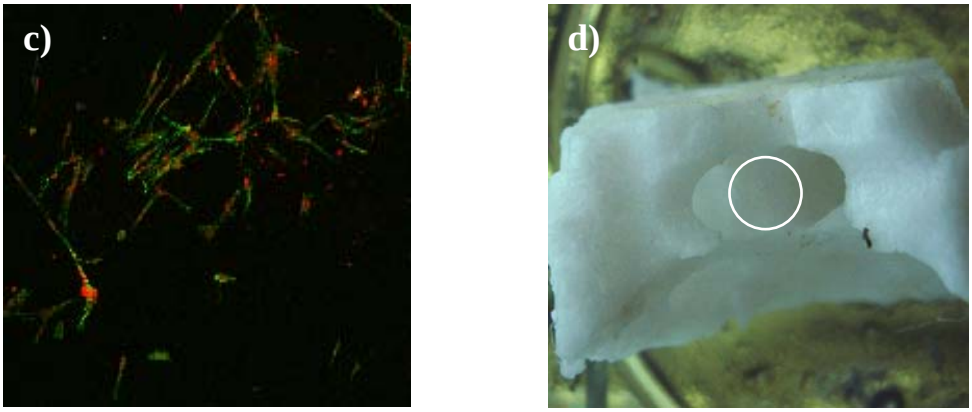

Figure 20 – CLSM images of cells cultured for 3 days on macroporous Bonelike® samples showing: (a) the surface sample covered with cells (20x); (b) the surface sample near a macropore, also covered with cells (10x); (c) a few cells in the interior of the macropores (10x); and (d) the spot from where the previous image was captured (Stereomicroscope image).

At day 7, the sample surface was covered by dense layers of cells. The black spaces observed in Figure 21a were due to surface irregularities of the sample analysed. Cells also migrated through macropores, but were not able to covered completely all the interior of the macropores (Figure 21c).

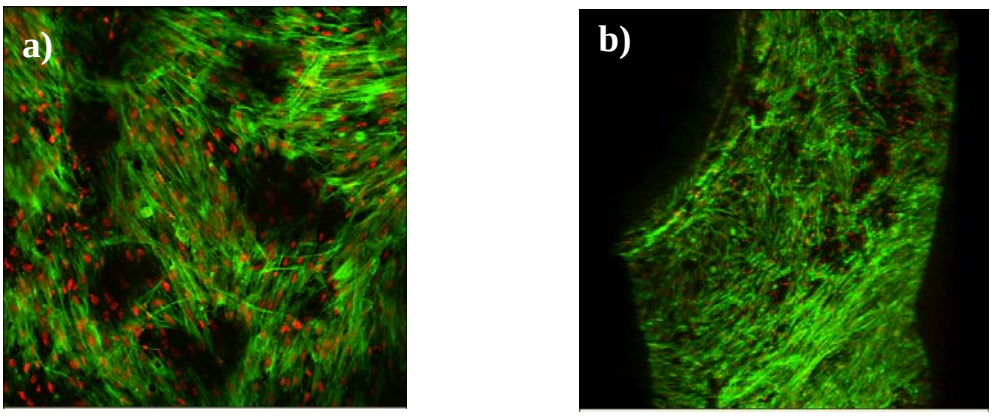

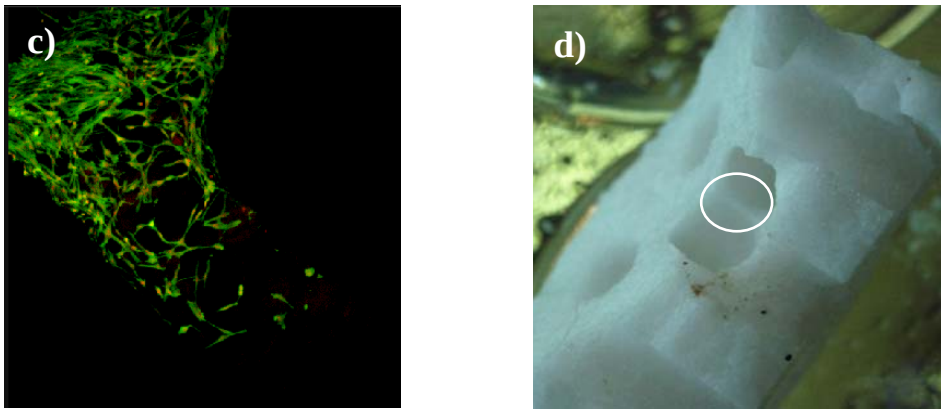

Figure 21 - CLSM images of cells cultured for 7 days on macroporous Bonelike® samples showing: (a) the surface sample covered by dense layers of cells (10x); (b) the surface sample near a macropore, also covered by dense layers of cells (10x); (c) cells in the interior of the macropores (10x); and (d) the spot from where the previous image was captured (Stereomicroscope image).

Next figures show the surface sample (Figure 22a) and the interior of macropores (Figure 22b and c) of day 14 sample completely covered by dense layers of cells.

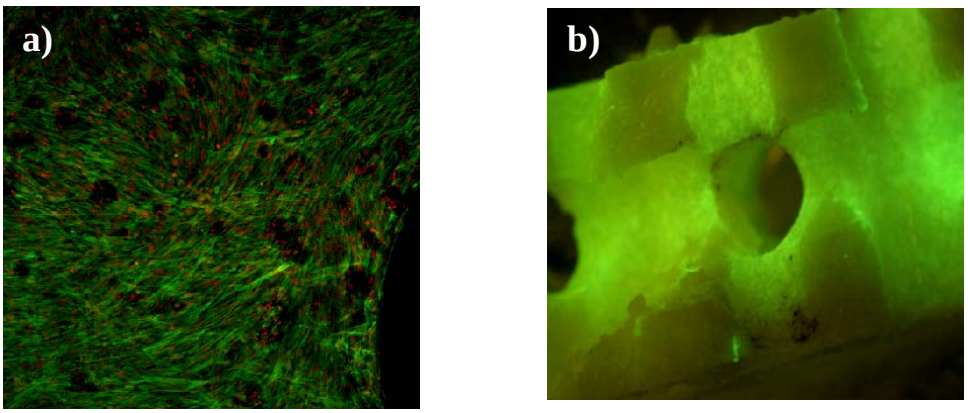

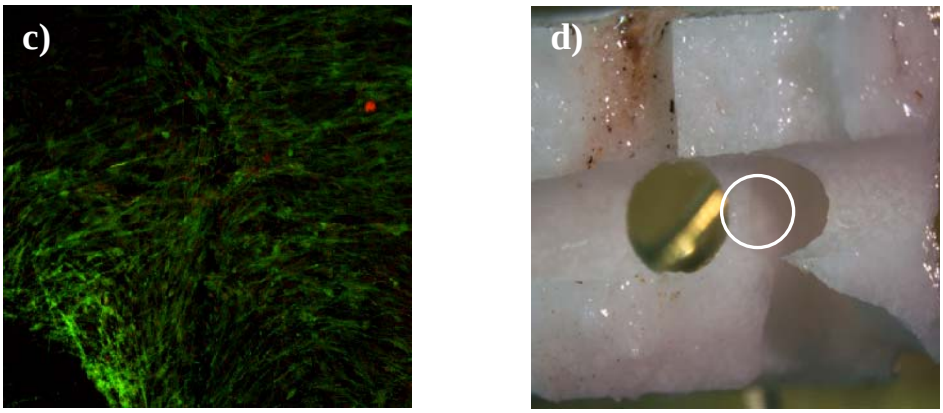

Figure 22 - Images of cells cultured for 14 days on macroporous Bonelike® samples showing: a) the surface sample near a macropore covered by dense layers of cells (CLSM image 10x); b) the interior of the macropores completely covered by cells (Stereomicroscope image with fluorescence); c) the interior of the macropore covered by dense layers of cells (CLSM image 10x) and d) the spot from where the previous image was captured (Stereomicroscope image).

At day 28 surface sample was covered by dense layers of cells. Interestingly, cells constructed bridges-like structures (Figure 23c) that in some cases covered all the macropore entrance (Figure 23a and b).

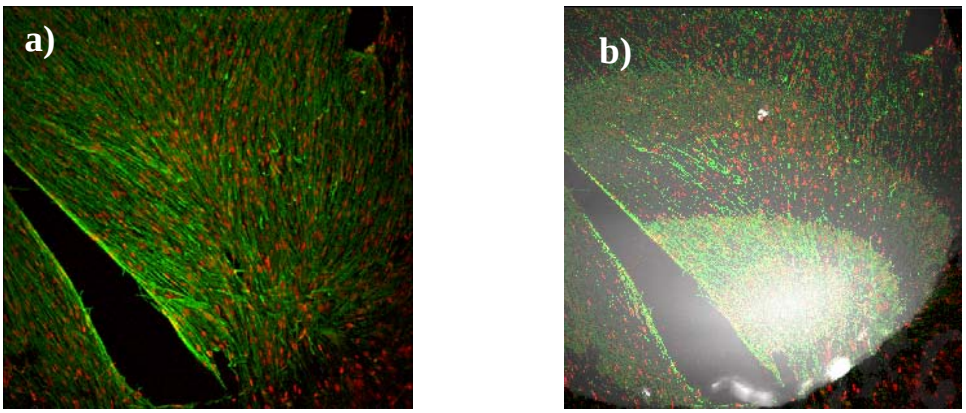

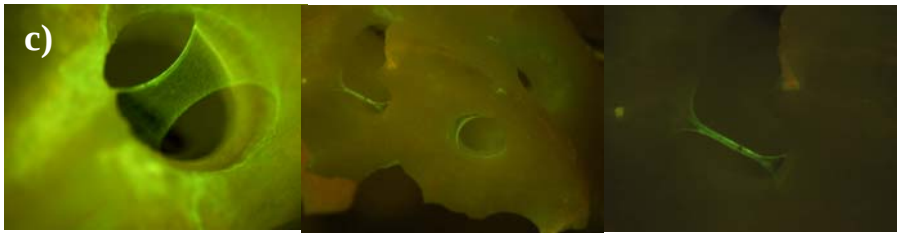

Figure 23 - Images of cells cultured for 28 days on macroporous Bonelike® samples showing: (a) and (b) the surface sample and macropore covered by dense layers of cells (CLSM image 10x); (c) cell bridges.

SEM analysis confirmed the observations by CLSM. Figure 24 shows the surface sample and internal surface of macropores covered by dense layers cells on samples cultured for 14 and 28 days.

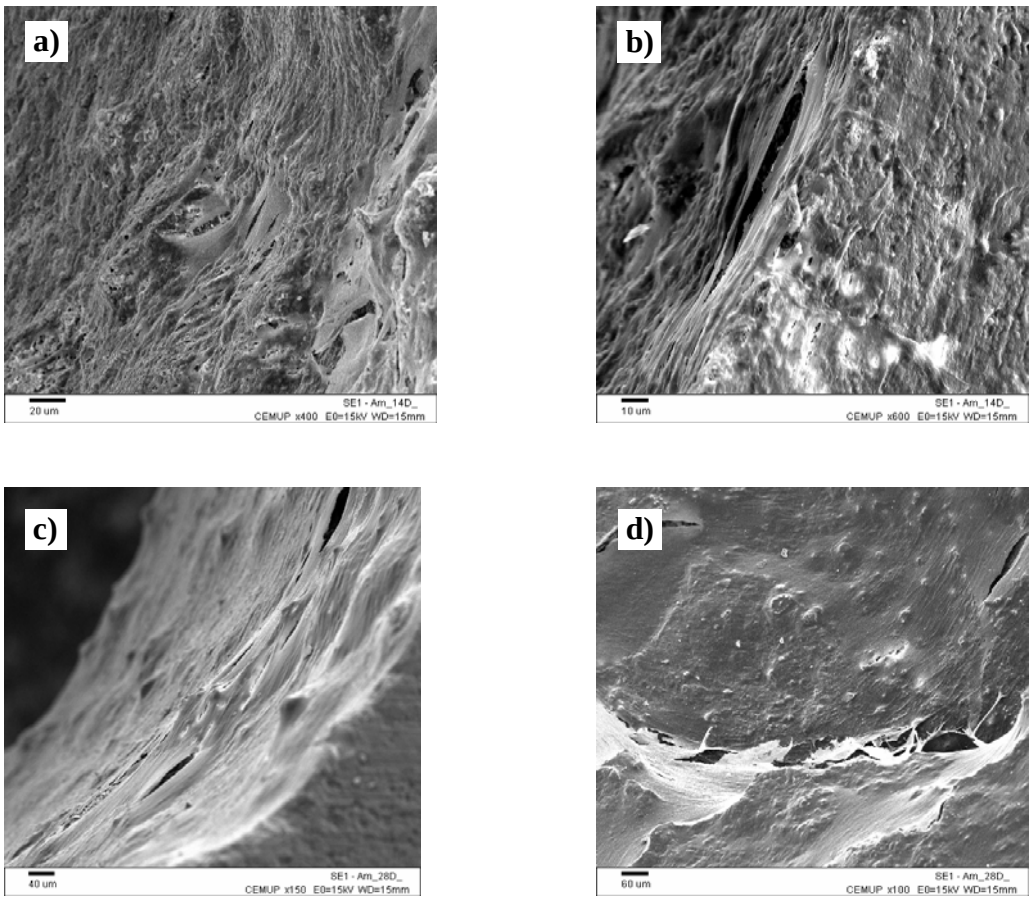

Figure 24 – SEM images of cells cultured on macroporous Bonelike® samples showing: day 14 sample (a) macropore and (b) surface covered by dense layers cells and (c) day 28 sample (a) macropore and (b) surface also covered by dense layers cells.

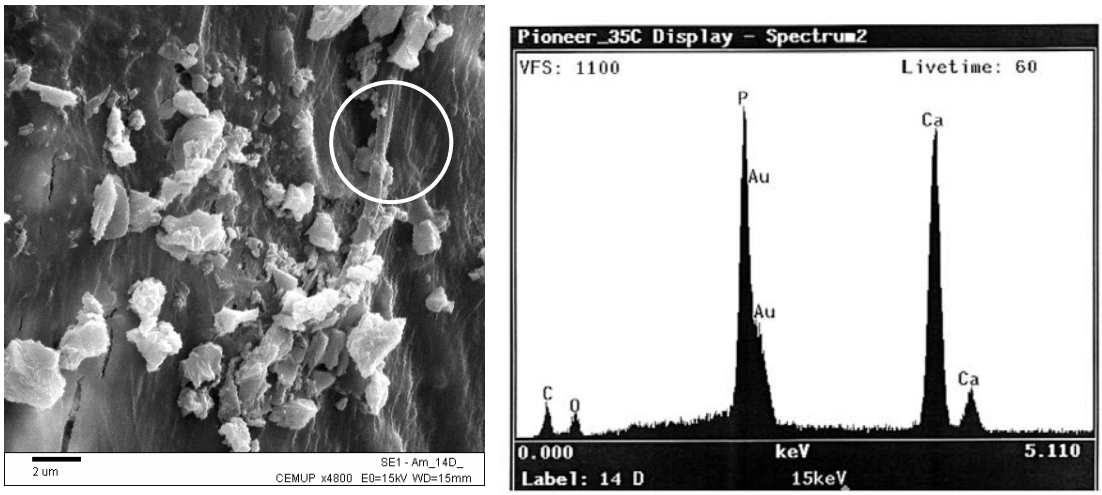

Figure 25 – SEM images of mineralized globular structures closed associated with cell layers cells cultured at day 14 sample and EDS spectrum.

Mineralized globular structures associated with cell layers were also identified (Figure 25). EDX spectrum of these structures showed the presence of Ca and P peaks. Cells were able to orient their growth (Figure 25b and c) according to the characteristic morphology of the surface sample and the internal surface of macropores.

DISCUSSION AND CONCLUSIONS

DISCUSSION

This thesis proposed the development of new bone repair scaffold using 3D biomodelling techniques. These scaffolds were prepared with a bioactive bioceramic, Bonelike®, which shows a chemical composition similar to the mineral bone [53, 54, 102]. On the other hand, 3D biomodelling allows the preparation of scaffolds with adequate size and shape to a specific implant site. The scaffolds prepared have controlled porosity with interconnected open pores.

The bioceramic powders prepared in laboratory were physico-chemical and structural characterized by different analytical techniques.

TCP phases were not detected in XRD spectra of sintered HA powders. On the other hand, Bonelike® spectra revealed the presence of the three phases (HA, β-TCP, α-TCP). It is referred to in literature [50, 53, 104, 105], that HA reacts with the glass added during the sintering process, and part of HA decomposes into β-TCP, and this last one inverts to α-TCP.

Several studies [6, 21, 49, 106] verified that glass reinforce composite reveal a higher densification comparing to HA. During the sintering process, densification occurred by liquid formation of the glassy phase which has a lower melting point compared to major phase, spreading all over the composite. Phosphate-based glasses bond to the solid HA particles and reduce the interfacial energy, eliminating porosity in the microstructure, one of the major causes of failure in the ceramics [6, 4, 22].

The composite microstructure is composed by HA and the TCP phases spread throughout the material, creating fully interpenetrated matrices of HA and TCP [107]. The toughness of the present phases in the composite is quite different, for example β-TCP is known to be much tougher (1.3 times) than HA [108]. In other ceramics like partially stabilised zirconia (PSZ), which consists of a mixture of zirconia and MgO, when phase transformation occurred from a metastable tetragonal to monoclinic phase, the volume of the precipitate increased [109].

The same mechanism has been proposed during the phase transformation of HA into β-TCP, and this last one to α-TCP, and a residual stress is created. The toughness contrasts of the phases, combined with expansions associated with phase transformation

of HA to the secondary phases, causes microcracking, [107, 108] which may lead to the loss of small parts of the material, leaving the correspondent cavities, obtained in this work. Furthermore, samples after being perforated and sintered showed large cracks all around the surface, next to sample border, so probably microcracking was much more extended in this kind of porous samples comparing with dense samples. However, macroporous 3D HA samples were also prepared using a CNC milling machine and it was verified that pure HA was not easy to machine. Comparatively, Bonelike® allow for the machinig, due to its higher mechanical properties.

FTIR spectra of HA revealed peaks of the functional groups OH^- and PO_4^{3-}, whose wavelengths are in according with literature [110]. The same peaks were found in Bonelike® spectra, although OH^- peaks underwent a significant decrease compared to HA. During the sintering process of Bonelike®, HA decomposes into TCP. Since TCP are not composed by the functional group OH^-, these ions were lost from HA lattice. At the same time, Ca/P ratio is altered since TCP Ca/P ratio is lower (1.5) comparing to the Ca/P ratio 1.67 of stoichiometric HA [47].

Several studies [47,111] verified that H_2O bands and OH^- peak were hardly detected in FTIR spectra of commercial HA samples sintered at 1300ºC. This could be due to the substitution of OH^- by O^{2-}. The final product of this reaction is the oxyhydroxyapatite [112, 113]. However, this process is reversible, and this apatite can react with H_2O present in the atmosphere during cooling furnace cycles and reincorporate some of OH^- and the H_2O [47] in order to lower its free energy. The dehydration and consequently lost of OH^- from HA is initiated around 600ºC and oxyhydroxyapatite start thereby to be formed [114]. .

Botelho *et al* [110] prepared HA in laboratory using the same precipitation chemical route, sintered it at 1300ºC, and the FTIR spectra of HA showed visible peaks of OH^- groups. The same was verified for HA spectrum of the present work. Possibly OH^- were reincorporated in HA lattice from the atmosphere, during cooling cycles as referred to above [47].

The second objective of this work was focused on the preparation of 3D Bonelike® macroporous structures, using a CNC milling procedure that removed the material according the virtual computer model. Samples prepared by this 3D machining

technique presented a homogeneous macropore distribution, previously modullated by adequated software's. It was ensured that all macropores were opened and interconnected. The porous scaffolds prepared by conventional techniques (salt particles) show a pore interconnection dependent of whether the adjacent particles are in contact. Most of the conventional methods used to prepare macroporous bioceramics has the disadvantage of using substances that may leave residues such as organic solvents (chloroform and methylene chloride), which may damage cells [117]. This milling process avoids this kind of contamination.

Concerning the material preparation procedure, Bonelike® has demonstrated a quite reasonable behaviour to the machining process, after being submitted to all steps of preparation described in chapter 2. However, cracks appear all around the surface, next to sample border as referred to above. The volume contraction of Bonelike® samples, that occurred after sintering, was not homogeneous, macropore contraction was higher than the distance between two consecutive pores.

Glass S.J. *et al* [116] agree that homogeneous densification is achieved when green compact are uniformly packed. Packing heterogeneities can be due to the presence of agglomerates of particles or pores leading to density variation. The densification in these cases is heterogeneous and the lower density regions can be physically constrained. In the same way, macropores of the samples prepared correspond to regions of lower densities suffering a higher volume shrinkage compared with material between macropores channels.

Also after sintering, macropores of approximately 2000 μm were obtained, larger than 100 μm the minimal size necessary for bone tissue ingrowths and regeneration, according with many studies [41,117]. Larger macropores can be advantageous allowing the circulation of water, nutrients and metabolic waste [32, 33].

In this work, the biological performance of Bonelike® samples was performed by using bone marrow stroma cells seeded on the surface of the material, in order to evaluate cell attachment, spreading, migration and growth through the 2000 μm macropores, as well as osteoblastic differentiation events.

Bone marrow stroma is an heterogeneous mixture of cells including adipocytes, reticulocytes, endothelial and fibroblast cells in contact with the hematopoetic elements.

It also contains cells that differentiate into bone, cartilage, fat and connective tissue which support the differentiation of hematopoietic cells [92,118].

Primary culture was obtained by culturing the bone marrow suspension in α-minimal essential medium supplemented with 10 % FBS. The selection of osteoprogenitor cells present in the bone marrow stroma was based on the ability of these cells to adhere on the surface of the culture plate. The majority of non-adherent cells such as erythrocytes and cells from hematopoietic lineage, were removed during the course of routine changing the medium [92, 118]. At 70 – 80 % confluence, i.e. in a stage of exponential cell growth, adherent cells were enzymatically released and the cell suspension obtained was seeded on the surface of the macroporous material samples. The seeded samples were cultured for 28 days and osteoblastic differentiation was elicited by ascorbic acid, dexamethasone and β-glycerophosphate. Ascorbic acid is essential for the production of the collagenous bone extracellular matrix, dexamethasone stimulate the differentiation of osteoblastic lineage cells and β-glycerophosphate is a source of phosphate ions required for the mineralization process [96, 97,119]. In this work, first-passage cells were used in the biological testing, since previous studies showed that sequential subculturing of bone marrow cell cultures results in a progressive loss of osteobastic differentiation parameters [96, 97].

Bonelike® samples colonized with osteogenic-induced bone marrow cells were observed by CLSM, Stereomicroscopy and SEM throughout the 28-day culture time. Cells were able to attach and spread on the surface of the Bonelike® samples. At early culture times, cells presented an elongated fibroblast-like morphology with a close interaction with the material topography and cell-to-cell contact. Few cells were also observed on the surface of the macropores. Cell growth rate was high, and cells migrate promptly to the macropores; at long incubation times (14 to 28 days), dense multilayers were observed, both on the surface and on the macropores internal surface, and also the presence of cell bridges connecting the macropores. SEM analysis revealed no evidence of cell bridges, which may be destroyed during the critical point proceeds. At days 14 and 28, SEM analysis showed mineralized globular structures containing calcium and phosphorous closed associated with cell layers, which may constitute a proof that cells were able to fully differentiate on the Bonelike® macroporous samples. In addition, cell

growth seemed to be guided by surface morphology. This was evident in the cell layer growing on the macropores surface, which presented a regular pattern resulting from the procedure used in the perforation of the material samples. This observation is in line with previous studies referring that cells can orient themselves according to the surface morphological patterns [36, 45, 120, 121].

The results regarding the cell behaviour observed in the present work are in agreement with previous *in vitro* biological studies performed in dense samples of Bonelike® with different compositions. It was observed that MG63 osteoblast-like cells presented a typical morphology, a high growth rate and expressed key extracellular matrix components (collagen type I, osteocalcin and fibronectin) [122-124], confirming that the physical and chemical surface characteristics of Bonelike® are adequate for cell development [125]. More recent studies evaluated the response of human osteoblastic bone marrow cells to Bonelike® (with fluoride ions in its composition) and showed that this material presented a better biological performance compared with HA, concerning the cell growth rate, alkaline phosphate activity and matrix mineralization [124,126,127].

Previous *in vitro* biological studies developed by A. Bignon *et al* were performed on porous calcium phosphate (70%HA and 30% β-TCP) with different macropore sizes prepared by a conventional technique, a porogen agent (polyvinyl butyral). The osteoblasts were able to migrate through the macropores by the emission of cytoplasmatic extensions and colonized the depth of the material. Thus, this colonization was easier in larger macropores (600-1250μm) with few interconnections [128]. E. Sachlos and J.T. Czernuszka agree that cell colonization is difficult in foam structures with uncontrolled porosity due to the diffusion foam constraints concerning cell migration and fluids [117]. Regarding the results of the present work, the scaffolds with large macropores seem to be very effective comcerning the cell migration into the interconnected channels.

It is difficult to extrapolate *in vitro* results to *in vivo* behaviour due to the differences between the two systems [129]. *In vitro* is not taken in account the immunological response of the organism, the neovascularization and the interactions between all types of cells and proteins involved in the bone regeneration. The *in vivo*

system is dynamic, with a continuous circulation of body fluids which prevent elevated ion levels at the cell/materials interface [129]. On the other hand, cell phenotype can be changed in long periods of cell culture, leading to false results.

In conclusion, bone marrow cells were able to migrate into all 2000 μm macropores of the 3D Bonelike® structures, as well as proliferate and differentiate along osteoblast lineage.

CONCLUSIONS

The main conclusions of this work may be described as follows:

The XRD analysis revealed the phase purity of the HA powder prepared in laboratory and Bonelike ® showed a controlled phase composition of HA, β-TCP and α-TCP. The HA reacted with the $CaO\text{-}P_2O_5$ glass during the liquid phase sintering process, and part of it decomposed into β-TCP and this last one inverts to α-TCP at higher temperatures [50, 53, 104, 105].

FTIR spectra of HA and Bonelike® revealed the same functional groups of OH^- and PO_4^{3-}. However, some OH^- were lost due to HA phase transformation into TCP [47].

After sintering, macropores of 3D Bonelike® samples underwent a higher contraction comparing to the distance between two consecutive pores, probably because they correspond to regions of lower density [116].

The 3D machining techniques, in this specific case the CNC milling machine, allowed for the control of different porosity parameters such as pore size, pore distribution and pore interconnections in opposite to conventional techniques used to prepare porous materials. Interconnected macropores with approximately 2000 μm pore size were obtained, larger than 100μm the minimal size necessary for cell migration, neovascularization and circulation of water, nutrients, gases and the removal of metabolic waste [37, 58, 61, 117].

Bone marrow cells were able to proliferate and migrated into all macropores of the 3D Bonelike® samples. For cells incubated for longer periods, ie 28 days, cells could form bridges and in some cases covered the macropore entrance. Mineralized globular structures associated with cell behaviour were identified, showing that complete differentiation of human bone marrow cells occurred on the surface of Bonelike®.

These results suggest that 3D structures with large macropores (2000 μm) interconnected channels allow for the success of cell migration into the interior of the Bonelike®.

REFERENCES

[1] Karlsson M. Nano-porous alumina, a potential bone implant coating. UppsalaUniversity, Uppsala, 2004.

[2] Van Wynsberghe D, Noback CR, Carola R. Bones and Bone tissue. In: Human Anatomy and Physiology. 3nd ed: McGraw-Hill, 2000.

[3] Hench LL, Best S. Ceramics, glasses, and glass-ceramics. In: Ratner BD, Hoffman AS, Schoen FJ, Lemons JE, editors. Biomaterial Science: An Introduction to Materials in Medicine. 2nd ed: Elsevier Academic Press, 2005.

[4] Blair HC, Zaidi M, Schlesinger PH. Mechanisms balancing matrix synthesis and degradation. Biochem J., 2002; 364:329-341.

[5] Marks SC, Hermey DC.The structure and development of bone. In: Bilezikian, J, Raisz, Rais Z, Rodan GA, editors. Principles of Bone Biology. Academic Press, 1996.

[6] Donahue JD, Siedlecki CA, Voggler E. Osteoblastic and osteocytic biology and bone tissue engineering. In: Hollinger JO, Einhorn TA, Doll BA, Sfeir C, editors. Bone Tissue Engineering. CRC Press, 2005.

[7] Fernandes MH, Mecanismos de regulação do metabolismo ósseo. Acta Médica Portuguesa, 1998; 11:41-52.

[8] Boskey AL. Mineralization, structure, and function of bone. In: Seibel MJ, Robins SP, Bilezikian JP. Dynamics of Bone and Cartilage Metabolism. Academic Press, 1999.

[9] Wopenka B, Pasteris JD. A mineralogical perspective on the apatite in Bone. Materials and Science Engineering, 2005;25:131-143.

[10] Aoki H. Science and medical applications of hydroxyapatite. Tokyo, Japan: Takayama Press,1991.

[11] Katz JL. Biomedical Engineering Fundamentals. CRC press, 2006.

[12] Wang C, Duan Y, Markovic B, Barbara J, Howlett CR, Zhang X, Zreiqat H. Proliferation and bone-related gene expression of osteoblast grown on hydroxyapatite ceramics sintered at different temperature. Biomaterials, 2004; 25: 2949-2956.

[13] Junqueira LC, Carneiro J. Histologia Básica. 7nd ed: Guanabara Koogan, 1990.

[14] Callis GM. Bone. In: Bancroft D, Garuble M, editors. Theory and practice of histological techniques, 5nd ed: Churchill Livingstone, 1990.

[15] Robey PG, Bianco P. Stem cells in tissue engineering. In: Lanza R, Blau H, Melton D, Moore M, Thomas ED, Verfaillie C, Weissman I, West M, editors. Handbook of Stem Cells. vol. 2, Elsevier, 2004.

[16] Bianco P, Riminucci M, Gronthos S, Robey P. Bone marrow stroma cells: Nature, Biology and Potential Applications. Stem Cells; 2001:19; 180-192.

[17] Dean RJ, Moseley A.B. Mesenchymal stem cells: Biology and potential clinical uses. Experimental Hematology,2000;28: 875-884

[18] Adapted from webschoolsolution.com/patts/systems/skeleton

[19] Adapted from bibliocean.com/OmniDefinition/bone

[20] Ducy P, Schinke T, Karsenty G. The osteoblast fibroblast under central surveillance. Science, 2000; 289: 0036-8075.

[21] Davies JE, Hosseini MM. Histodymanic of endosseous wound healing. In: Davies JE, editors. Bone engineering, Toronto: em^2, 2000.

[22] Blair HC, Zaidi M, Schlesinger PH. Mechanisms balancing skeletal matrix synthesis and degradation. Biochem. J., 2002; 364:329-341.

[23] Braddock M, Houston P, Campbell C, Ashcroft P. Born again bone: Tissue engineering for bone repair. News Physiol. Sci., 2001; 16:0886-1714/99

[24] Kalfas IH, Houston P, Campbell C, Ashcroft P. Principles of bone healing. Neurosurg. Focus, 2001;10: article 1.

[25] Botelho CM. Silicon-substituted Hydroxyapatite for Biomedical Applications. Faculdade de Engenharia da Universidade do Porto, 2004.

[26] Toquet J, Rohanizadeh R, Guicheux J, Couillaud S, Passuti N, Daculsi G, Heymann D. Osteogenic potencial in vitro of human bone marrow cells cultured on macroporous biphasic calcium phosphate ceramic. J Biomed Mater Res, 1999; 44: 98-108.

[27] Williams DF. Progress in Biomedical Engineering 4-Definitions in Biomaterials. Elsevier Academic Press, 1987.

[28] Dias AG. Biodegradable Glass Ceramics for Bone Regeneration. Faculdade de Engenharia da Universidade do Porto, 2004.

[29] Tadic D, Epple M. A thorough physicochemical characterisation of 14 calcium phosphate-based bone substitution materials in comparison to natural bone. Biomaterials, 2004; 25: 987-994.

[30] Goldberg V, Stevenson S. Natural history of autografts and allografts. Clinical Orthopaedics & Related Research,1987; 225: 7-16.

[31] Salgado JA, Coutinho OP, Reis RL. Bone tissue engineering: state of the art and future trends. J Biomed Mater Res, 1999; 44: 98-108.

[32] Temenoff JS, Mikos AG. Injectable biodegradable materials for orthopaedic tissue engineering. Biomaterials, 2000; 21: 2405-2412.

[33] Hulmatcher DW, Schantz T, Zein I, Ng KW, Teoh SH, Tang KC. Mechanical properties and cell cultural response of polycaprolactone scaffolds designed and fabricated via fused deposition modelling. J Biomed Mater Res, 2001; 55:203-216.

[34] Hutmacher DW. Scaffolds designed and fabrication techniques for tissue engineering tissues – state of the art and future perspectives. J Biomater. Sci. Polymer Edn, 2001; 12:107-124.

[35] Anselme K.Osteoblast adhesion on biomaterials. Biomaterials, 2000; 21:667-661.

[36] Bo-Yi Y, Pei-Hsun C, Yi-Ming S, Yu-Tsang L, Tai-Horng Y. Topological micropatterned membranes and its effect on the morphology and growth of human mesenchymal stem cells (hMSCs). Journal of membrane science, 2005; 273:31-37.

[37] Hollister SJ, Maddox RD, Taboas JM. Optimal design and fabrication of scaffolds to mimic tissue properties and satisfy biological constraints. Biomaterials, 2002; 23: 4095-4103.

[38] Heungsoo S, Seongbong J, Antonios GM. Biomimetic materials for tissue engineering. Biomaterials, 2003; 24: 4353-4364.

[39] Hutmacher DW. Scaffolds in tissue engineering bone and cartilage. Biomaterials, 2000; 21: 2529-2543.

[40] Rhee JM, Scott DB. Opportunities in spinal applications. In: Hollinger JO, Einhorn TA, Doll BA, Sfeir C, editors. Bone Tissue Engineering, CRC Press, 2005.

[41] Hench LL, Wilson J. Introduction. In: Hench LL, Wilson J, editors. An introduction to bioceramics, World Scientific, 1993.

[42] de Aza PN, de Aza S. Biocerámicas. In: Sastre R, de Aza S, Róman JS, editors. Biomateriales, World Scientific, 1993.

[43] Bajpai PK, Billotte WG. Ceramic biomaterials. In: Bronzino JD, editors. The biomedical engineering Handbook, CRC press, 1995.

[44] Ravaglioli A, Krajewski A. Bioceramics: Materials, properties, applications. Chapman & Hall, 1992.

[45] Rosa A, Belotia MM, van Noortb R. Osteoblastic differentiation of cultured rat bone marrow cells on hydroxyapatite with different surface topography.
Dental materials, 2003; 19: 768- 772.

[46] Liua D, Yanga Q, Troczynskia T, Tsenga JW. Structural evolution of sol–gel-derived hydroxyapatite. Biomaterials, 2002; 23: 1679- 1687.

[47] Santos JD. Development of Hydroxyapatite-glass composites for biomedical applications. Faculdade de Engenharia da Universidade do Porto, 1993.

[48] Khon MJ, Rakovan J, Hughes JM. Phosphates: Geochemical, geobiological, and materials importance. Mineralogical Society of America, 2002.

[49] Lopes MA, Monteiro FJ, Santos JD.Glass-reinforced hydroxiapatite Composites: Secondary Phase Proportions and Densification Effects on Biaxial Bending Strength. J. Biomed Mater Res (Appl Biomater), 1998; 48: 734-740.

[50] Georgiou G, Knowles JC. Glass-reinforced hydroxyapatite for hard tissue surgery – Part 1: mechanical properties. Biomaterials, 2001;22: 2811-2815.

[51] Duarte F, Santos JD, Afonso A. Medical applications of Bonelike® in Maxillofacial Surgery. Material Science Forum, 2004; 455-456: 370-373.

[52] Prado da Silva MH, Lemos AF, Gibson IR, Ferreira JM, Santos JD. Porous glass reinforced hydroxyapaite materials produced with different organic additives. Journal of Non-Crystalline Solids, 2002; 304: 286-292.

[53] Lopes MA, Santos JD, Monteiro FJ, Knowles JD. Glass-reinforced hydroxiapatite: A comprehensive study of the effect of glass composition on the crystallography of the composite. J. Biomed Mater Res., 1998; 39: 244-251.

[54] Queiroz AC, Santos JD, Monteiro FJ, Gibson IR, Knowles JC. Adsorption and release studies of sodium ampicillin from hydroxyapatite and glass-reinforced hydroxyapatite composites. Biomaterials, 2001; 22 : 1393-1400(2001).

[55] Queiroz AC, Santos JD, Monteiro FJ, Prado da Silva MH. Dissolution studies of hydroxyapatite and glass-reinforced hydroxyapatite ceramics. Materials Characterization, 2003; 50: 197-202.

[56] Queiroz AC, Teixeira S, Santos JD, Monteiro FJ. Porous Hydroxyapaitite for controlled Release of Sodium Ampicillin. Key Engeneering Materials, 2004; 254-256:997-1000.

[57] www.therics.com/therics-products/.

[58] Leong KF, Cheah CM, Chua CK. Solid freeform fabrication of three-dimensional scaffolds for engineering replacement tissues and organs. Biomaterials, 2003; 24: 2363–2378.

[59] Wilson CE, de Bruijn JD, van Blitterswijk CA, Verbout AJ, Dhert WJA. Design and fabrication of standardized hydroxyapatite scaffolds with a defined macro-architecture by rapid prototyping for bone-tissue-engineering research. J. Biomed Mater Res, 2004; 68A: 123–132.

[60] Simske SJ, Ayers RA, Bateman TA. Porous materials for bone engineering. In: Liu D, Dixit V, editors. Porous materials for tissue engineering, Trans Tech Publications, 1998.

[61] M. Bohner, G.H. van Lenthe, W. Hirsiger, R. Evison, R. Muller, "Synthesis and characterization of porous β-tricalcium phosphate blocks", Biomaterials,26, 6099-6105 (2005).

[62] Sous M, Bareille R, Rouais F, Clément D, Amédée J, Dupuy B, Baquey C. Cellular biocompatibility and resistance to compression of macroporous β-tricalcium phosphate ceramics. Biomaterials, 1998; 19: 2147-2153.

[63] Arita IH, Castano VM. Synthesis and processing of hydroxyapatite ceramics tapes with controlled porosity. Journal of Materials Science: Materials in Medicine, 1995; 6: 19-23.

[64] da Silva MP, Lemos A, Ferreira JM, Santos JD. Mechanical Characterization of Porous Glass Reinforced Hydroxyapatite Ceramics – Bonelike®. Materials Research, 2003; 6: 0-0.

[65] White RA, Webwe JN, White EW. Replamineform: a new process for preparing porous ceramic, metal, and polymer prosthetic materials. Science, 1972; 176:922-924.

[66] Roy DM, Linnehan SK. Hydroxyapatite formed from natural coral skeletal carbonate by hydrothermal exchange. Nature, 1974-, 247: 220-222.

[67] Lin FH, Liao CJ, Chen KS, Sun JS, Lin CY. Preparation of β-TCP/HAP biphasic ceramics with natural bone structure by heating bovine cancellous bone with addition of $(NH_4)_2HPO_4$). J Biomed Mater Res, 2000; 51: 157-163.

[68] Tancred DC, McCormack BA, Carr AJ. A synthetic bone implant macroscopically identical to cancellous bone. Biomaterials, 1998-, 19: 2303-2311.

[69] Lee LJ , Zeng C, Cao X, Han X, Shen J, Xu G. Polymer nanocomposite foams. Composites Science and Technology, 2005; 65: 2344-2363.

[70] Sepulveda P, Ortega FS, Innocentini MDM, Pandolfelli VC. Properties of highly porous hydroxyapatite obtained by the gelcating of foams. Journal of the americam ceramic society, 2000; 12: 3021-3024(4).

[71] Nam Y, Yoon JJ, Park T. A Novel Fabrication Method of Macroporous Biodegradable Polymer Scaffolds Using Gas Foaming Salt as a Porogen Additive. J. Biomed Mater Res(Appl Biomater), 2000; 53: 1-7.

[72] Haugen P, Ried V, Brunner M, Will J, Wintermantel E. Water as foaming agent for open cell polyurethane structures. Journal of Materials Science: Materials in Medicine, 2004; 15: 343-346.

[73] Lu D. Fabrication of hydroxyapatite ceramics with controlled porosity. Journal of Materials Science: Materials in Medicine, 1997; 8: 227-232.

[74] Tadic D, Beckmann F, Schwarz K, Epple M. A novel method to produce hydroxyapatite objects with interconnecting porosity that avoids sintering. Biomaterials, 2004; 25:3335-3349.

[75] Leatrese DH, Byung-Soo K, David JM, Higa OZ. Open pore biodegradable matrices formed with gas foaming. J. Biomed Mater Res, 1998; 42: 396-402.

[76] Fabbri M, Celotti CG, Ravaglioli A. Hydroxyapatite-based porous aggregates: physico-chemical nature, structure, texture and architecture. Biomaterials, 1995;16: 225-228.

[77] Woesz A, Rumpler M, Stampf J, Varga F, Fratzl-Zelman, Roschger P, Klaushofer K, Fratzl P. towards bone replacement materials from calcium phosphates prototyping and ceramic gelcasting. Materials science and Engineering, 2005; 25C:181-186.

[78] D'Urso PS, Atkinson RL, Weidmann MJ, Redmond MJ, Half BI, Farwaker WJ, Thompson RG, Effeney DJ. Biomodelling of skull base tumours. Journal of Clinical Neuroscience, 1999; 6(1): 31-35.

[79] Qingbin L., Leu MC, Schmitt SM. Rapid prototyping in dentistry: technology and application. Int J Adv Manuf technol, 2005.

[80] Santos JD *et al*. Projecto de investigação científica e desenvolvimento tecnológico (FCT) POCTI/CTM/59091/2004 - "Nova Geração de Biomateriais Biactivos e Bioreabsorvíveis para cirurgia regenerativa do tecido ósseo utilizando biomodelação 3D".

[81] Alves FG, Braga FG, Simão M, Neto RJ, Duarte TM. Prototipagem rápida. Protoclick!,2001.

[82] Burns, M. Automated fabrication: improving productivity in manufacturing. Prentice Hall, 1993.

[83] Pham DT, Gault RS. A comparison of rapid prototyping techniques. Int Jrnl of Machine Tools and Manufacture, 1998; 38: 1257-1287.

[84] Leatham-Jones B. Introduction to computer numerical control, Longman, 2001.

[85] Valentino JV, Goldenberg J. Introduction to computer numerical control (CNC), 3nd ed, Person Education, 2003.

[86] [3d biomod 4] Chu MG, Orton DG, Hollisten SJ, Feinberg SE, Halloran JW. Mechanical and in vivo performance of hydroxyapatite implants with controlled architectures. Biomaterials, 2002; 23: 1283-1293.

[87] Pahole I, Drstvensek I, Ficko M, Balic J. Rapid prototyping processes give new possibilities numerical copying techniques. Journal of materials processing technology, 2005; 164-165: 1416-1422.

[88] Anselme K. Osteoblast adhesion on biomaterials. Biomaterials, 2000; 21: 667-681.

[89] Alberts B, Bray D, Johnson A, Lewis J, Raff M, Roberts K, Walter P. Essential cell biology: An introduction to the molecular biology of the cell. Garland Publishing, Inc, 1998.

[90] Microsoft Encarta. Microsoft Corporation, 2004.

[91] Ferreira MN, Correia MO. Ciclo celular. In: Azevedo C, editor. Biologia celular e molecular. 4nd ed: Lidel, 2005.

[92] Freshney RI. Basic principles of cell culture. In: Freshney RI, vunjak-Novakovic G, editors. Culture of cells for tissue engineering. 5nd ed: Wiley-Liss, 2000.

[93] Freshney RI. Culture of animal cells: A manual of basic techniques. 5nd ed: Wiley-Liss, 2000.

[94] Bruder SP, Caplan AI. Bone regeneration through cellular engineering. In: Lanza P, Langer R, Vacanti J, editors. Principles of tissue engineering. 2nd ed: Academic Press, 2000.

[95] Bareille R. General aspects and technical issues of cells culture methods. In: 7th advanced summer course in cell-materials interactions – Regenerative Medicine; Porto, Portugal, 2006.

[96] Coelho MJ. Modulação farmacológica da interacção tecidos ósseo/biomateriais – Estudos *in vitro*. Faculdade de Medicina Dentária da Universidade do Porto, 2001.

[97] Costa MA. Modulação da osteogénese em culturas de osso alveolar humano. Faculdade de Medicina Dentária da Universidade do Porto, 2000.

[98] www.weizmann.ac.il/Chemical_Research_Support//EM_Unit/

[99] Fonseca PS. Introduction to confocal microscopy and it applications to stuffy cell-material interactions. In: 6th advanced summer course in cell-materials interactions – At molecular level; Porto, Portugal, 2005.

[100] Adapted from www.qubic.com.au/roland_mdx20_15.htm

[101] Adapted from www.rolanddg.com/product/3d/3d/mdx-20_15/mdx-20_15.html

[102] Lopes MA, Knowles JC, Santos JD. Structural insights of glass.reinforced hydroxyapatite composites by Rietveld refinement. Biomaterials, 2000; 21: 1905-1910.

[103] Salih V, Georgiou G, Knowles JC, Olsen I. Glass reinforced hydroxyapatite for hard tissue surgery part II: in vitro evaluation of bone cell growth and function. Biomaterials, 2001; 22: 2817-2824.

[104] Lobato J, Hussain S, Botelho CF, Maurício A, Afonso A, Ali N, Santos JD. Assessment of Bonelike Graft with a Resorbable Matrix Using an Animal Model. Thin Solid Films, 2006:515; 362-367.

[105] Landi E, Tampieri A, Mattioli-Belmonte M, Celotti G, Sandri M, Gigante A, Fava P, Biagini G. Biomimetic Mg- Mg, Co3-substituted hydroxyapatite synthesis, characterization and in vitro behaviour. Journal of the European Ceramic society, 2005, in press.

[106] Santos JD, Knowles JC, Reis RL, Monteiro FJ, Hasting GW. Microstructural characterization of Glass-reinforced HA composites. Biomaterials, 1994:15; 5-10.

[107] Tancred DC, McCormack BAO, Carr AJ. A quantitative study of the sintering and mechanical properties of hydroxyapatite/phosphate glass composites. Biomaterials, 1998:19; 1735-1743.

[108] Lopes MA, Monteiro FJ, Santos JD. Glass reinforced HA composites: fracture toughness and hardness dependence on microstructural characteristics. Biomaterials, 1999:20; 2085-2090.

[109] Smith WF. Princípios de Ciência e Engenharia dos Materiais. 3nd ed: McGraw-Hill, 1998.

[110] Botelho CM, Lopes MA, Gibson IR, Best SM, Santos JD. Structural analysis of Si-substituted hydroxyapatite: zeta potencial and x-ray photoelectron spectroscopy. Journal of materials science: Materials in Medicine, 2002:13; 1123-1127.

[111] Oliveira JM, Miyazaki T, Lopes MA, Ohtsuki C, Santos JD.Bonelike®/PLGA hybrid materials for bone regeneration: Preparation route and physicochemical characterisation. Journal of materials science: Materials in medicine, 2005:16; 253-259.

[112] Ducheyne P. Bioactive Ceramics. J. Bone Joint Surg, 1994:76; 861-4.

[113] Gross KA, Berndt CC, Stephens P, Dinnebier. Oxyapatite in hydroxyapatite coating. Journal of materials science, 1998:33; 3985-3991.

[114] Shen Z, Adolfsson E, Nygren M, Goan L, Kawaoka H, Niihara K. Dense hydroxyapatite-Zirconia ceramic composites with strength for biological applications. Adv Mater, 2001:13; 214-216.

[115] Rehman H, Bonfield W. Characterization of hydroxyapatite and carbonated apatite by photo acoustic FTIR. Journal of materials science: materials in medicine, 1997:8; 1-4.

[116] Glass SJ, Mahoney FM, Gwsuk KG. Ceramic powders compactation. In: American society International Symposium on Manufacturing Practices and Technology; New Orleans, EUA, 1995.

[117] Sachlos E, Czernuszka JT. Making tissue engineering scaffolds work review on the application of solid freefrom fabrication technology to the production of the tissue engineering scaffolds. European Cells and Materials, 2003; 5: 29-40.

[118] Baksh D, Song L, Tuan RS. Adult mesenchymal stem cells: characterization, differentiation, and application in cell and gene therapy. J. Cell. Mol. Med., 2004; 3 : 301-316.

[119] Coelho MJ, Fernades MH. Human bone marrow cells in biocompatibility testing. Part II: effect of ascorbic acid, β-glycerophosphate and dexamethasone on osteoblastic differentiation. Biomaterials, 2000; 21:1095-1102.

[120] Ratner BD, Hoffman AS. Physicochemical surface modification of materials in medicine. In: Ratner BD, Hoffman AS, Schoen FJ, Lemons JE, editors. Biomaterial Science: An Introduction to Materials in Medicine. 2nd ed: Elsevier Academic Press, 2005.

[121] Lincks J, Boyan BD, Blanchard CR, Lohmann CH, Lui Y, Cochran DL, Dean DD, Schwartz Z. Response of MG63 osteoblast-like cells to titanium and titanium alloy is dependeny on surface roughness and composition. Biomaterials, 1998; 19: 2219-2232.

[122] Lopes MA, Knowles JC, Kuru L, Santos JD, Monteiro FJ, Olsen I. Flow cytometry for assessing biocompatibily. J Biomed Mat Res, 1998; 41: 649.

[123] Lopes MA, Knowles JC, Santos JD, Monteiro FJ, Olsen I. Direct and indirect effects of P2O5-glass-reiforced hydroxyapatite on the growth and function of osteoblast-like cells. Biomaterials, 2000; 21: 1165.

[124] Hussain NS, Lopes MA, Maurício AC, Ali N, Fernandes MH, Santos JD. Bonelike ® grafts for bone regenerative applications. In: Ahmed W, Jackson MJ, editors. Surface engineered biomedical and surgical devices`.

[125] Ferraz MP, Fernandes MH, Santos JD, Monteiro FJ. HA and double layer HA-P_2O_5/CaO glass coating: influence of the chemical composition on human bone marrow cells osteoblastic behaviour. Journal of material science: Materials in medicine, 2001; 12: 629-638.

[126] Costa Ma, Gutierres M, Almeida R, Lopes MA, Santos JD, Fernandes MH. In vitro mineralisation of human boné marrow cells cultured on Bonelike®. Key. Eng. Mater., 2004; 821: 254-256.

[127] Costa MA, Gutierres M, Almeida R, Lopes MA, Santos JD, Fernandes MH. In vitro mineralisation of human bone marrow cells cultured on Bonelike®. Key. Eng. Mater., 2004; 821: 254-256.

[128] Bignon A, Chouteau J, Chevalier J, Fantozzi G, Carret JP, Chavassieux P, Boivin G, Melin M, Hatmann D. Effect of micro- and macroporosity of bone substitutes on their mechanical properties and cellular response materials. Journal of materials science: materials in medicine, 2003; 14; 1089-1097.

[129] Dias AG, Lopes MA, Trigo Cabral AT, Santos JD, Fernandes MH. In vitro studies of calcium phosphate glass ceramics with different solubility using human bone marrow cells. Journal of biomedical materials research, 2005; 74: 347-355.